Journal of Hydrology 617 (2023) 128873

Contents lists available at ScienceDirect

Journal of Hydrology

journal homepage: www.elsevier.com/locate/jhydrol

Research papers

Long-term climatological and ecohydrological analysis of a paired catchment – flux tower observatory near Dresden (Germany). Is there evidence of climate change in local evapotranspiration?

T. Pluntke [a,1,*], C. Bernhofer [a,1], T. Grünwald [a], M. Renner [b], H. Prasse [a]

[a] Chair of Meteorology, Institute of Hydrology and Meteorology, Department of Hydro Sciences, Faculty of Environmental Sciences, Technische Universität Dresden, 01069, Germany

[b] Brandenburg State Office of Environment, State Hydrological Service/ Flood Monitoring Center, Müllroser Chaussee 50, 15236 Frankfurt, Germany

ARTICLE INFO

This manuscript was handled by Marco Borga, Editor-in-Chief

Dedicated to the memory of Uwe Eichelmann, an exceptional technician-scientist.

Keywords:
Catchment water budget
Eddy-covariance
Forest evapotranspiration
Climate change
Land surface change
ICOS

ABSTRACT

Water budgets and climate are related in many ways and at all scales. Therefore, we expect climate change to trigger changes in all water budget components at any scale. For Central Europe observed and projected climate change indicates higher variability of precipitation, while evapotranspiration (ET) should increase due to higher temperatures, yielding lower and more variable infiltration and runoff. However, evidence in ET records is limited, as long-term measurements of ET are methodologically challenging and as factors other than climate are changing in parallel, like vegetation and land use.

In this study, we take advantage of long-term hydro-meteorological data from the small research catchment Wernersbach (4.6 km^2, dominated by Norway spruce) in operation since 1967 and from two eddy-covariance (EC) flux towers, all located in the Tharandt Forest, Germany. The tower DE-Tha is located a few kilometres east of the catchment, is spruce dominated and in operation since 1996. After a wind break of a spruce stand (situated inside the catchment) and planting of deciduous oaks, the tower DE-Hzd was set up in 2009. For the first time, we report systematically about observation, correction methods and metadata of the long data series of the observatory, represented by the Wernersbach catchment and the EC flux towers.

Climate change signals in the region are mirrored in the Tharandt Forest records. They show rising air temperature with a breakpoint around 1988 and complex changes in solar radiation associated to a regional peak in air pollution around the same time. The catchment and both towers did not show any systematic differences in climate or meteorological data, allowing us to address observed changes in the water budget components as related to (i) climate change, (ii) change in vegetation, and (iii) different responses due to different soil and hydrogeological characteristics as well as methodological aspects. The catchment term ET plus storage, derived from precipitation minus runoff, showed the expected high variability with a significant increase over the more than 50 years of operation. The flux-tower DE-Tha showed much lower inter-annual variability in ET with an average annual total of 486 mm (1997 to 2019), but no significant trend. For the same period, average catchment ET was 734 mm/yr. The younger flux-tower DE-Hzd showed ET values in between, closer to catchment ET at the very dry end of the ten-year record (2010 to 2019). An analysis of decadal trends in a Budyko framework at catchment level revealed the dominating response of ET to land use or vegetation change until around 1990. The climate induced change of ET increased in the last decades, on the one hand directly due to an increased atmospheric demand. On the other hand, extreme weather events exerted harmful effects on vegetation, especially triggered by two dry years at the end of the record.

Furthermore, we found that the mean annual tower ET was about 250 mm lower than catchment ET despite the careful correction for energy balance closure. We attribute this difference to soil and to a lesser extend to vegetation characteristics, but also to methodological uncertainties. There is evidence from interception and transpiration measurements at the flux tower as well as from water budget modelling that a major contribution of this difference is related to an insufficient EC closure correction during interception events. A careful

* Corresponding author at: Technische Universität Dresden, Faculty of Environmental Science, Institute of Hydrology and Meteorology, Chair of Meteorology, 01062 Dresden, Germany.

E-mail address: thomas.pluntke@tu-dresden.de (T. Pluntke).

[1] Made equal contributions.

https://doi.org/10.1016/j.jhydrol.2022.128873
Received 22 April 2022; Received in revised form 4 November 2022; Accepted 19 November 2022
Available online 30 November 2022

consideration of rain events and evaporation from interception is recommended when addressing ET of similar evergreen forests in a humid climate, as EC records might be generally too low. This illustrates the necessity of redundant and complementary measurements when dealing with large system complexity.

1. Introduction

Climate change and its possible effects on the water budget is of increasing concern among environmental scientists as well as among decision makers (WWDR, 2020). Expected shifts towards higher temperatures, higher evapotranspiration (ET) and higher variability in precipitation (IPCC, 2014) would lead to lower and/or more variable runoff and eventually lower groundwater recharge. Climate change thus threatens freshwater resources (Bates and Kundzewicz, 2008). However, water and land management will often hide these effects especially for large catchments with many competing factors of influence (Bates and Kundzewicz, 2008). This adds to the general delay in catchment response to atmospheric drivers due to storage effects. Thus, trends in discharge and ET cannot be attributed to climate change alone, as other effects influence the system response (Kundzewicz et al., 2013).

However, for small catchments with an unchanged land cover and land management, a warming climate should lead to an increase of ET or at least, a change of ET we can understand from non-climatic effects, like forest management (e.g., Arbeitskreis KLIWA et al., 2018). Therefore, additional information on non-climatic drivers of the water balance is crucial when we investigate catchment response to climate change.

The area of investigation is the Tharandt Forest, a large (60 km^2) managed forest dominated by spruce stands (about 2/3 of the forest) south-west of Dresden, the capital of Saxony (Germany). The time period covered is 1968 to 2019. Climate change is already remarkably evident in Central Europe. A temperature increase of 1.5 K and a shift towards less frequent but more intense precipitation events are observed (Bates and Kundzewicz, 2008; IPCC, 2014) increasing the risk of floods and droughts (Bernhofer et al., 2006). In Saxony, this pattern is most pronounced in summer. The start of the warming trend can be associated to a regional breakpoint around 1988 (Renner and Bernhofer, 2011). Seasonally only fall contributed a bit less to this trend (Bernhofer et al. 2015). Regional and local changes in precipitation are always subject to uncertainty due to the large temporal and spatial variability of precipitation. However, a decrease of late spring precipitation (Apr/May/Jun) and an increase in late summer (Jul/Aug/Sep) were observed consistently relative to 1961–1990. According to precipitation sums, the occurrence and intensity of heavy precipitation decreased in late spring and increased in late summer, a fact which might aggravate hydrological droughts in both seasons (Bernhofer et al. 2015). At the end of the period under investigation, a serious drought occurred (2018/19/20) with an accumulated deficit relative to normal conditions of around 400 mm throughout Saxony. This drought was driven by low precipitation and high air temperature, leading to high vapour pressure deficit and high evaporative demand (Pluntke et al., 2021).

Additionally, the regional climate was affected by air pollution. Since the 1960 s, large sulphur dioxide emissions from fossil fuel burning led to a high aerosol density in the upper troposphere reducing the global (or solar) radiation via scattering over most of Europe and North America. While this effect was reduced by filtering the emissions elsewhere in the early 1980 s, leading to a “global brightening” (Philipona et al., 2009), it continued in neighbouring parts of today’s Germany, Poland, and Czech Republic (the so called “Black Triangle”, see e.g., Kolář et al. 2015) until the early 1990. Please note that this “regional brightening” (i) shows a delay of about ten years relative to the global effect and (ii) was accelerated by the fast reductions of emissions, at least in Saxony.

In higher elevations of the Black Triangle, a severe forest dieback occurred due to this heavy air pollution and the associated deposition. This caused a reduction in forest cover and forest vitality between 1970 and 1990 with effects on the water budget. Discharge increased for most forested catchments in the area. Renner et al. (2014) disentangled the typical land use/land cover (LULC) changes from climate change to show these hydro-climatological consequences for a large set of catchments in Saxony. After curbing the sulphur dioxide emissions in the early 1990 s and the following regrowth of the forest, by 2010 forest conditions and catchment response had almost returned to conditions before 1960.

Other typical LULC changes in the area included water management of agricultural areas (drainage of wet areas, but also irrigation) and changes in field size and cropping system due to the use of heavy machinery and the move to large agricultural units (cooperatives). Even forested areas were often drained to improve growth. After 1990, some of the monospecific spruce forests were managed towards a larger proportion of deciduous trees, like beech or oak. Therefore, we should expect complex responses of the hydrological system depending on the LULC and its management as well as depending on regional and global climate change.

This study focusses on the catchment Wernersbach (WB) and two accompanying flux towers. The WB catchment is a small, forested research catchment (Dyck and Peschke, 1995; Bernhofer 2002, 2018) with a data record starting in 1967. This catchment was much less affected by the sulphur dioxide deposition than the forests close to the border of the Czech Republic. This is due to the lower elevation, lower wind speed, and lower exposure to the emissions. It is completely forested mostly by spruce since at least 100 years, and no larger reservoirs or agricultural activities had been recorded. Such small experimental catchments with a single land use and long-term monitoring (climate, hydrology, management) offer the chance to single out climate effects.

Since 1996 an eddy covariance (EC) flux tower monitors energy, water and carbon fluxes in the same area above an old, managed forest dominated by spruce (Grünwald and Bernhofer, 2007). In the ICOS network (Alam et al., 2019) the identifier is DE-Tha, which will be used also in this study. 2009/10, additionally the flux tower “Hetzdorf” DE-Hzd went into operation. This tower is within the catchment and collects flux data from a growing young oak forest after a wind break in 2007. EC based flux networks like FLUXNET (Baldocchi et al., 2001), ICOS or NEON enlarged our understanding of the global carbon cycle (Fernández-Martínez et al., 2017; Petrescu et al., 2015), but also provide insight into the terrestrial energy and water balance (Teuling et al., 2010; Yao et al., 2016), including disturbances like droughts (Graf et al., 2020; Teuling et al., 2013).

Only a few studies exist on co-located catchments with appropriate measurements of precipitation and runoff, and flux towers with EC based flux measurements of ET, like the pioneering comparison of catchment vs tower ET by Amiro and Wuschke (1987) or the multi-site study of Teuling et al. (2013). The only long-term data set with some similarity we are aware of is the Rietholzbach catchment (Seneviratne et al., 2012) in the Swiss Alps. However, the Rietholzbach catchment is grassed and a weighing lysimeter provides ET. Comparisons for much shorter periods of three to five years were published (Graf et al., 2014; Kosugi and Katsuyama, 2007) and showed mostly good agreements of catchment and flux tower ET. For the catchment WB and the flux tower DE-Tha Frühauf et al. (1999) found a good correspondence between both ETs for the water budget year 1997/98. Teuling et al. (2013) deduced from the combination of WB and DE-Tha, and soil moisture estimates of the GRACE satellite that low precipitation and high ET can occur simultaneously at catchment level, as long as the storage component is sufficiently large.

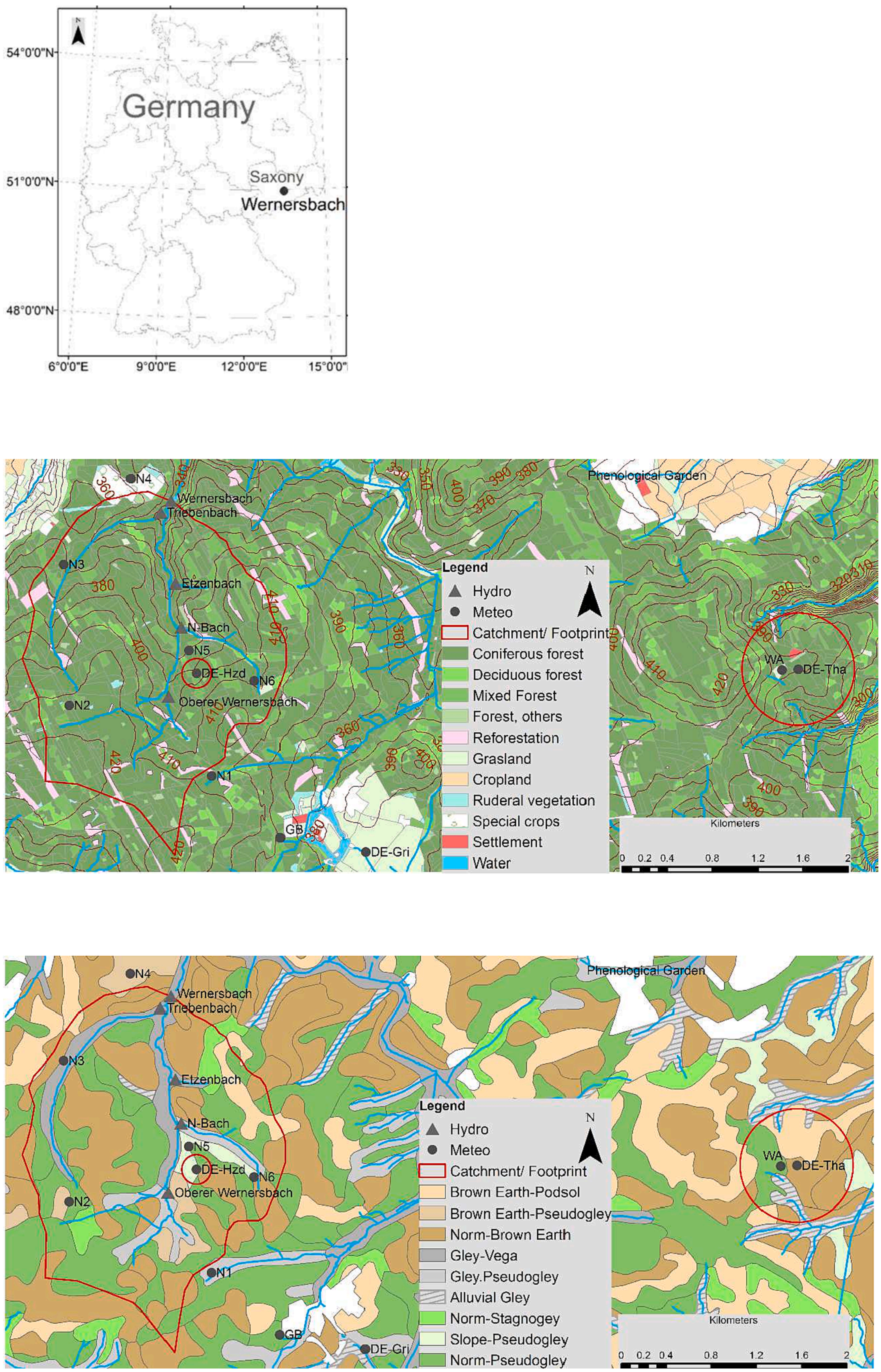

Fig. 1. Study area relative to Germany (upper panel), land use (2005), elevation, catchment of WB, footprint area of the EC towers, meteorological and hydrological measurement sites at WB and nearby (central panel) as well as soil types (lower panel, for abbreviations see Appendix B). Soil information is based on data from the Saxon State Office for Environment, Agriculture and Geology.

Table 1
Share of dominant soil sub-types in WB, DE-Hzd and DE-Tha and relevant soil parameters: skeletal fraction SKV (average) and usable field capacity (UFC) within the rooting depth.

NUM	Code	Soil sub-type	Share in DE-Tha (%)	Share in WB (%)	Share in DE-Hzd (%)	SKV (Vol %)	UFC *1 (mm)
291	SSg	Slope-Pseudogley	1 %	1 %	49 %	39	145
294	GG-SS	Gley-Pseodogley	0 %	6 %	0 %	20	125
265	SSn	Norm-Pseudogley	0 %	22 %	23 %	8	178
279	GG-AB	Gley-Vega	0 %	10 %	0 %	24	268
261	BBn	Norm-Brown Earth	12 %	21 %	28 %	31	185
543	BBn	Norm-Brown Earth	19 %	4 %	0 %	75	76
346	SSn	Norm-Pseudogley	19 %	8 %	0 %	4	162
295	BB-PP	Braun Earth-Podsol	20 %	0 %	0 %	80	83
531	Gga	Alluvial Gley	10 %	0 %	0 %	40	133

*1 Usable field capacity at pF 1.8 for the profile until 1.2 m or the potential rooting depth.

The major research question of the study is, whether a response of actual ET to observed climate change can be identified. To answer this question, we have to test the data for consistency including a careful evaluation of the ET monitoring techniques, potential methodological bias of ET and to sort out other factors like storage or land management. This leads to the following objectives: (i) to investigate the long-term data of the catchment WB (52 years) and the flux tower DE-Tha (23 years) for the dynamics in the water and energy budget components, (ii) to analyse short-term dynamics of ET and storage and its contribution for the evolution of droughts, (iii) to attribute ET changes to land use and climate changes, respectively, and (iv) to check on the respective representativeness of the co-located research sites, WB and the EC flux towers DE-Tha and DE-Hzd.

2. Location, measurements and methods

2.1. Location

2.1.1. General information and geology

The WB catchment is situated in the Tharandt Forest at the low elevations of the Erzgebirge/Ore Mountains in Saxony/ Germany (Fig. 1). The small river or creek WB is a tributary of the river Triebisch which itself drains into the river Elbe in Meissen. The WB is about 3 km long, and small tributaries are *N*-Bach, Etzenbach and Triebenbach. The catchment size is 4.6 km^2. If not additionally specified, information on the catchment refers to the complete WB watershed, regardless of, e.g., different runoff or infiltration characteristics within the catchment. For a characterisation of the EC towers, a reference area is assigned to each tower (footprint according to Mellmann et al., 2003; Kljun et al., 2004). The footprint is not static, but for simplicity, we choose a typical daytime footprint according to EC measurement height and canopy structure. As a result, a fixed area is used within a 500 m radius around DE-Tha and 130 m around DE-Hzd tower.

Geologically, the catchment belongs to the Ore Mountains (Erzgebirge) and consists of the volcanic rock Palaeorhyolite, which is strongly fissured in its upper zone. Palaeorhyolite weathers cohesively causing a cementation of the fissures. Cretaceous sandstones from the Elbe valley deposited on top of the Rhyolite, but they can be found only in the peripheral areas of the catchment nowadays. In the western part of WB, these sandstones are tilted, likely causing a groundwater flow to the adjacent catchment. A reduction of the below surface catchment size by about 0.2 km^2 is commonly assumed (Müller, 1998). The topography is characterized by pronounced small scale heterogeneity with mainly gentle slopes (40 % $<1^\circ$, 54 % between 1 and 3°). Height above sea level ranges from 323 to 420 m (mean 388 m).

2.1.2. Soil types

Spatial distribution of soil types is shown in Fig. 1 and some characteristics are summarized in Table 1. Information is based on the soil map 1:50 000 of the Saxon State Office for Environment, Agriculture and Geology. Crucial soil characteristics, which determine the ET dynamics, are the skeletal fraction (SKV, grain fraction 2–200 mm) and the usable field capacity (UFC) of the soil profile at root level. SKV was averaged over the whole soil profile, with a weighing according to layer depth.

Dominant soil type in WB is Norm-Brown Earth, which developed over Rhyolite rocks (according to World Reference Base for Soil Resources: Albeluvisols). Typically, they have high infiltration rates. The alluvial zones and some neighbouring areas are groundwater and backwater influenced. There, they changed to gley (Gleysols) and pseudo-gley soils (Stagnosols, Planosols). Gley soils are often saturated leading to fast direct runoff after precipitation events. Generally, the soils in WB show a relative high water retention capacity (mean UFC over all relevant soil types having at least a share of 10% is 210 mm, see Table 1) and low infiltration rates (SKV 21 vol%).

At DE-Tha, the dominating soil types are Norm Brown Earth and Brown Earth Podsol, which have high infiltration rates, and Norm Pseudogley, which is a backwater influenced soil with low infiltration rates. Overall infiltration is better but water retention capacity is worse than in WB, which is reflected by a UFC of 127 mm and SKV of 48 vol%. The dominant soil type in the footprint of the tower DE-Hzd is Slope-Pseudogley (backwater influenced soil), two soil types of DE-Hzd are also common in WB. The SKV is slightly higher (26 vol%) and the UFC lower (169 mm) than in WB.

2.1.3. Land cover and land use

The main land cover in the WB catchment is coniferous forest. According to data of the 1980 s, Norway spruce (*Picea abies*) was dominating (35 % in pure stands and 47 % in mixed stands), accompanied by 12 % Scots pine (*Pinus sylvestris*) in mixed stands and a minor portion of deciduous and coniferous species. Forest management has changed throughout the period covered here. Three main clear-cutting periods took place in 1965–1970, 1978–1981 and 1985–1988, before clear-cutting was practically abandoned. In 2007, a larger area was subject to a severe wind storm damage. After removing the spruce stems, a deciduous stand was planted with two oak species (*Quercus rubra, Quercus robur*) in 2008. As this offered the unique opportunity to study the effects of a disturbance, a micrometeorological tower including EC was set up to monitor the dynamics at the regrowth site in 2010 (DE-Hzd).

The tree species distribution at WB and DE-Tha has been very similar until today. However, the Saxon Forest management is slowly converting these forest stands from spruce dominated to mixed stands at this elevation. The spruce forest at DE-Tha was established by a special seeding technique called *Plätzesaat* in 1887 that already uses seedlings instead of seeds. Further replanting took part in 1890, 1891 and 1899. However, a tree ring analysis of four spruce trees in September 2020 arrived at ages between 114 and 118 years, which shows a small discrepancy to the official seeding date. In the footprint of the EC tower, the forest was composed of 87 % coniferous and 13 % deciduous trees in 1999 (Appendix A). The understory consists mainly of *Fagus sylvatica* (20 %, planted) and *Deschampsia flexuosa* (50 %). The young beeches had been introduced to mirror the typical forest management of Saxony

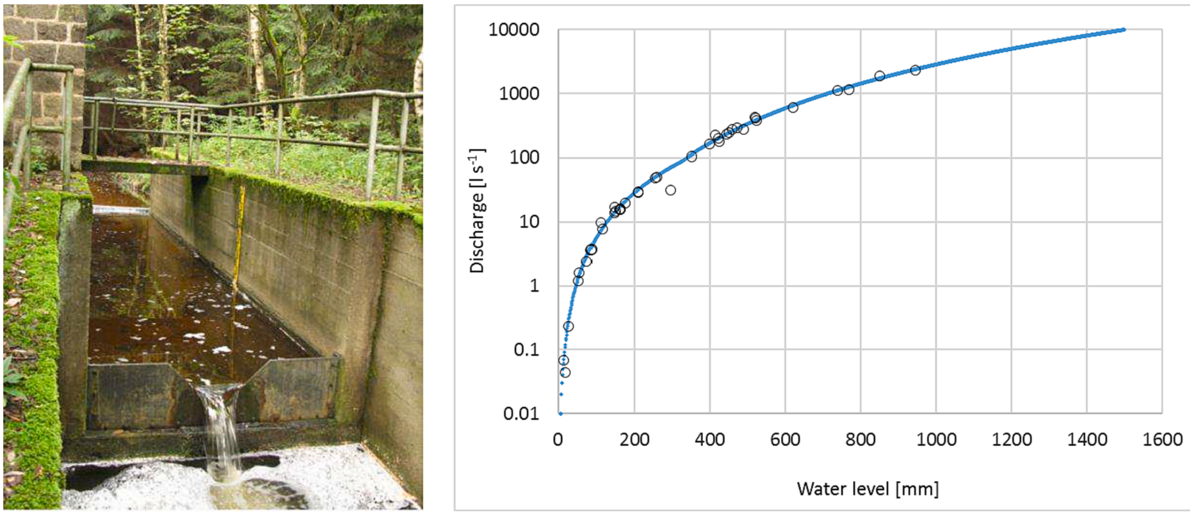

Fig. 2. Left: Thompson weir at the outlet of WB. Right: measurements of water level and discharge (open circles) and the resulting rating curve (blue). (For interpretation of the references to colour in this figure legend, the reader is referred to the web version of this article.)

aiming at a more resilient species composition. Forest management at DE-Tha also included thinning of the old stand (2002, 2011, and 2016). Recently, white fir (*Abies alba*) has been introduced as an additional species in the understorey. Appendix A gives an overview of the development of land cover over time of all three sites. Comparisons between inventories are hampered, because only in 2013 non-forested areas were quantified and understorey is not considered in each inventory. The apparent increase in spruce in DE-Tha from 2013 to 2019 and the decrease in deciduous trees originates from the latter issue. In reality, beech is growing as understorey here. Nevertheless, trends towards more deciduous trees are recognizable at all three sites.

2.1.4. *Climate and climate change*

In Germany, the climate is oceanic according to Köppen-Geiger (type Cfb, Kottek et al., 2006). Cfb represents a warm temperate year-round humid and summer warm climate. The continental influence increases from NW to E. Saxony is consequently more continental. At WB the mean temperature was 7.7 °C (Grillenburg) and the yearly precipitation sum corrected for wind loss was 921 mm/yr (1968–2019). The driest month was April 2007 with 0.3 mm and the wettest month August 2002 with 397 mm. The main part of the Tharandt Forest including WB is characterized by a gentle topography and a considerable variation in microclimate. Cold air pooling can lead to freezing temperatures close to the ground in any time of the year. Wind and precipitation are influenced as well by small scale orography.

There is a clear trend to higher temperatures in all seasons, but no clear effect on annual precipitation. However, there is evidence for precipitation changes in Saxony that differ between seasons (Hänsel et al. 2009). The first part of the summer half year (Apr-May-Jun) shows reduced precipitation, while the second part (Jul-Aug-Sep) was slightly wetter. This is in accordance with a positive trend of heavy precipitation (Schaller et al., 2020).

2.1.5. *Hydrologic characterisation*

The hydrological response of the WB catchment was associated to four hydrologically distinctive area types (Peschke et al., 1999): (i) 16 % are wet and saturated areas along the creeks, which form direct flow, (ii) 3 % are areas with dominant hypodermic flow, well connected to the creek, which form direct and hypodermic flow, (iii) 39 % are backwater influenced areas with soils of low infiltration rates but high water retention, barely connected to the creek, and (iv) 42 % are infiltration areas, which form base flow. A drainage system was created in the 1960 s to improve the site conditions for forest production. The drainage system was serviced until 1990 only. Therefore, over the past 30 years drainage should have slowly returned to smaller values, decreasing runoff.

2.2. *Measurements*

In December 1967, measurements started at the catchment WB, while the flux towers were in full operation only by 1996 (DE-Tha) and 2010 (DE-Hzd), respectively. All data (meteorological, hydrological and metadata) are stored in an internal database of the Chair of Meteorology. No initial harmonization was performed. In case of instrumental changes, overlapping observations are stored separately. For this work, daily data were prepared, which includes checks on homogeneity, homogenization and gap filling (see below). Practically all time-series consist of data with different equipment and site characteristics. Recent and historic instrumentation and further metadata are documented in Appendix B. As an example and as support in teaching, a subset of the data is released in parallel to this paper (see chapter 6). It consists of monthly hydro-meteorological data of the period 1968–2019, and an exemplary daily dataset of the year 2017 of WB and the data of the two EC towers. Generally, EC data are available via the European Fluxes Database Cluster (http://www.europe-fluxdata.eu/), the ICOS Carbon Portal (https://www.icos-cp.eu/) and the global FLUXNET initiative (https://fluxnet.org/), e.g., the FLUXNET2015 dataset was described in Pastorello et al. (2020).

2.2.1. *Wernersbach catchment*

The WB catchment was established by Hermann Pleiβ (first holder of the Chair of Meteorology at TU Dresden) for education and research within the former Faculty of Forestry between 1965 and 1967. The main outlet of the WB catchment is defined by a Thompson weir with a 90° V-notch and a width/ total height/ notch depth of 200 cm/ 90 cm/ 40 cm, respectively. Bypass-flow is blocked by a concrete wall across the valley floor perpendicular to the creek. The weir defines the catchment size, which was estimated to be 4.6 km^2. Discharge or runoff (R) is computed from water level (mechanical recording and additionally with a pressure sensor since February 1992) at the weir using the rating curve (water level - discharge relationship) as depicted in Fig. 2. Observations were manually corrected in case of clogging or ice formation. Discharge measurements by a flow meter (various propeller velocimeters; OTT or similar) were performed regularly to establish the rating curve, but thereafter additional measurements were done only on demand (esp. at high discharges). Later, it was checked again on special occasions, like after the summer floods in 1980 and in 2002.

Extreme floods transport considerable amounts of sediments. In August 2002, the two upstream sections of the weir were filled with about 3 to 4 m^3 of sediments along with the peak discharge. In 2018 on the occasion of the 50th anniversary of the WB, the complete weir including the concrete wall and the bypass channel were renovated. An ultrasonic sensor to detect the water level and a second ultrasonic sensor for flow velocity were installed for a continuous recording of the water level – discharge relationship by 2019. Main power was available at the weir until 1990. It was re-established in 2021 and allows a continuous sediment and water quality monitoring.

Five Hellmann precipitation (P) gauges (200 cm^2) were installed in December 1967 in and close to WB (see N1 through N6 in Fig. 1) in order to capture the spatial variation. To reduce wind induced errors, Tretyakov shields were installed in 1974. Recording rain gauges with higher temporal resolution were installed additionally in 1969/1972 (siphoning recorders), tipping bucket rain gauges in 1995 and a weighing gauge in 2003. Daily values are collected from the Hellmann gauges and temporally distributed according to the recorder values during post-processing. Episodic re-location of rain gauges became necessary due to growing trees in the vicinity to avoid shading effects. Typically, parallel measurements at the old and the new site were performed for some period of time to check for consistency.

Precipitation observations of Hellmann gauges were corrected for the typical losses: wetting and evaporation loss according to Karbaum (1969) and wind induced loss according to Richter (1995). As the types of rain gauges changed over time, as well as site conditions and manual reading frequency were not always according to standards, the corrections had to be adjusted. These gauges were Zinc-coated until November 2002 and were replaced by stainless steel gauges later. Wetting loss for Zinc-coated Hellmann rain gauges was corrected by adding 0.15 mm per precipitation event. Evaporation loss from the collecting vessel was corrected: in spring and autumn 0.05 mm, in winter 0 mm and in summer 0.1 mm per day for the period from the first precipitation event until the observation (three times per week). Depending on the exact start of the rain event and the time of observation, calculation is carried out with an accuracy of half a day. If necessary, half the surcharge is added. Before the installation of wind shields in February 1974, the Tretyakov shields were tested against measurements at the forest clearing close to the EC tower DE-Tha (WA). Little need for additional correction was found. Therefore, after the installation of wind shields, no wind correction was applied. For Hellmann gauges from stainless steel (in use since 2002) the total correction (note: here only wetting and evaporation loss) is generally 5.5 %. This factor was determined from long-term parallel observations at the Chair of Meteorology in Tharandt.

In wintertime (October through April) between 1968 and 1988, and 1990/91 the Hellmann gauges in WB were partly filled with brine to minimize losses due to evaporation and wetting. Snow detection improved as the concentrated solution melted the snow and the resulting water was less sensible to further wind loss. A thin film of petroleum at the surface of the liquid reduced evaporation errors. To arrive at precipitation, the volume and density of the liquid were determined. However, results did not drastically improve despite the effort, but gave a general picture of the associated bias.

Areal precipitation for the whole catchment is calculated as the arithmetic mean of available reliable stations according to the careful judgement of trained personal. From December 1967 until April 1990 stations N1-N5 were available, until December 1992 N1-N6, until December 1999 N2, N3, N5 and N6, until October 2008 N1, N2, N3, N5 and N6 and since then N1-N5.

Temperature (T) observations are available for the complete period from the forest clearing WA (part of DE-Tha) and from Grillenburg GB. Both data series are complete. GB is used for further analysis, because it is very close to the catchment and almost standard conditions prevail.

Wind speed (WS) is available from GB above grassland, at WA from a 19 m tower until 1996 and at DE-Tha at 33 m and 42 m (both heights are above canopy). None of the stations cover the complete period. To get a consistent time series for WB is challenging, because of different site characteristics and measuring heights. The station with the most similar condition to the forested WB is DE-Tha. Therefore, the time series at 42 m was gap-filled via a regression with the DWD station Dresden-Klotzsche (1972–2019). Remaining missing values were filled with mean daily values (of a yearly cycle), where a Gaussian white noise was added.

Relative Humidity (RH) is observed at GB since 1968, but a gap of several years exists in the 1980 s and 1990 s. The gap was filled using minimum temperature observations (adapted Magnus approach from Murray, 1967). The quality of this procedure is good as a cross validation shows with a coefficient of determination of $R^2 = 0.89$. The sensor has a drift since 2010, i.e., 100 % is never reached. This typical error was corrected applying a de-trending approach according to Körner et al. (2020).

Global radiation (RG) measurements at the top of the observation towers in DE-Tha and at WA were used. For consistency, parallel measurements were performed with each new sensor or at the beginning of the operational measurements at the new tower. When necessary, observations were corrected and referenced to the current radiation sensor (Kipp & Zonen CNR1/CNR4) using linear regression models. Largest differences exist between first measurements at WA (with an analogue recorder and manual analysis for daily and hourly values) and the following digital records at DE-Tha ($R^2 = 0.95$).

At the flux tower DE-Tha, net radiation (Rn) was measured by a Schulze net radiometer (Dr. Lange, Germany), short- and longwave radiation were separated using a combination with a Sonntag pyranometer (Lambrecht, Göttingen, Germany) at DE-Tha until 2007. Since 2007, a four-component net-radiometer (Kipp & Zonen CNR1/CNR4) is used. Inconsistencies were found in a later analysis only. To avoid misleading bias, the record was adjusted to the recent data. This procedure increased net radiation systematically before 2007, increasing the energy balance closure gap of the early years of DE-Tha. The closure corrected latent heat flux increased on dispense of a slightly increased uncertainty, as the correction of Rn is based on the assumption of constant site conditions.

Groundwater level measurements were available from three sites in the catchment (Müller, 1998); two sites are still in operation. Site 1 represents the conditions of the upper part of Oberer Wernersbach and reacts fast after precipitation events. Site 3 is situated at the ridge between Triebenbach and Wernersbach and is representative for a large groundwater storage, leading to considerable damping of the surface signal.

Soil water content was measured with a neutron probe (S-23) at 13 sites in the catchment, generally every 10 cm until a depth of 100 cm from 1970 to 2000. Tensiometers were used additionally close to the tributary *N*-Bach between 1991 and 2001. Today, inside the catchment, at DE-Hzd, four sites are probed regularly by FDR and TDR devices.

2.2.2. *Measurements at the flux towers*

All surface energy budget components including net radiation, soil heat flux, storage related fluxes, as well as turbulent heat fluxes are measured at two towers, one within WB at the oak regrowth site (DE-Hzd), the other one is the long term ICOS spruce site (DE-Tha) close to the catchment. Sensible and latent heat, momentum, as well as water vapour (H_2O), and carbon dioxide (CO_2) fluxes are determined using the eddy-covariance (EC) technique.

The flux tower at the spruce site was established for an investigation on forest decline in the early 1990 s. The rising interest in the carbon balance of forests led to the EUROFLUX project, which established the first continent wide network of EC stations including Tharandt (Valentini et al., 2000). The EC measurements started in DE-Tha in July 1996, establishing the longest continuous EC record of water and carbon exchange in Germany. The site DE-Hzd was added in 2010. Various additional information is available from the literature (e.g., Moderow and Bernhofer, 2014) and via the international cooperation in ICOS ERIC (https://www.icos-cp.eu/) or FLUXNET (https://fluxnet.org/).

The DE-Tha setup at 42 m above ground includes ultrasonic anemometers (GILL-*R*3, GILL-HS, Gill Instruments Lymington, UK) and closed-path gas analysers (LI-6262, LI-7000, LI-7200, LiCor Inc., Lincoln, NE, USA) (Bernhofer et al. 2003, Grünwald and Bernhofer, 2007). At DE-Hzd, EC measurements started at a height of 5 m above ground using an ultrasonic anemometer (CSAT, Campbell Scientific ltd., Logan, Utah, USA) and an open-path infrared gas analyser (LI-7500, LiCor Inc., Lincoln, NE, USA). Due to the growing forest the EC measurement level has been increased to 12 m/17 m above ground in 2017/2021. Details of the setups are given in Grünwald and Bernhofer (2007). The post-processing of fluxes follows the ICOS standard (Sabbatini et al., 2018) and FLUXNET procedures (Pastorello et al., 2020) including flux correction, quality control, footprint calculation, flux partitioning, gap filling, and correction for energy balance closure gap. The EC towers and their surroundings are equipped to collect additional meteorological (precipitation, radiation components, temperature, humidity), soil (ground heat flux, moisture, temperature), and biomass (diameter at breast height, litter fall, LAI, sap flow, leaf area and mass data, at DE-Tha also nutrients at leaf level) data.

2.3. Methods

2.3.1. Water budget method

ET of WB can be determined as a residual of the water budget over a multi-year integration time (P minus R). For shorter integration periods, groundwater, soil, and snow storage cannot be neglected, introducing a considerable challenge. In the following we will refer to this term as catchment ET. To understand the short-term dynamics of ET and storage and its contribution for the evolution of droughts, we applied an approach according to Teuling et al. (2013). It is based on the water balance of a catchment.

$$P = R + dS + ET \tag{1}$$

with precipitation *P*, net discharge or runoff *R,* change in catchment water storage (mainly by changes in soil moisture) *dS* and evapotranspiration *ET*. All terms in Eq. (1) are mass flux densities in kg $m^{-2}s^{-1}$ or mm d^{-1} for convenient comparison with precipitation standards.

In terms of anomalies (see Teuling et al. 2013), it can be written as

$$dS' - dS_0 = \int (P' - R' - ET')\, dt \tag{2}$$

where dS_0 is an arbitrary integration constant. From Frühauf et al. (1999) and hydrological reasoning, we know that a balanced soil water status was typically reached in late winter or early spring (March or April). Despite this we choose to use the hydrological year starting at November 1st for the purpose of better acceptance in the hydrological community. Climatological values of the water balance components, i.e., mean monthly values of the period 1997–2019 were calculated and used for anomaly calculations.

2.3.2. Eddy-covariance method

At the flux towers, the eddy-covariance method yields direct measurements of the turbulent fluxes above canopy. Typical formulation for ET is given as

$$ET_{EC} = \rho_a \overline{w'q'} \tag{3}$$

ρ_a is air density, w is vertical wind speed, q stands for specific humidity, ‘ denotes the deviation of the instantaneous value from the mean and the overbar the mean of a methodologically reasonable time period. For mostly pragmatic reasons, a frequency of 20 Hz and a half-hourly time period is commonly applied. The method is the state-of-the-art approach (i.e., the new standard) to measure turbulent energy and matter transport between the surface and atmosphere (Aubinet et al. 1999). This is associated to the surface energy balance of an “ideal site”, as shown in Eq. (4).

$$Rn - G - J = AE = H + L.ET \tag{4}$$

On the left side of Eq. (4), Rn stands for net radiation, G for ground heat flux, and J for the flux total due to storage changes between the measurement levels of net radiation and soil heat flux (Bernhofer et al. 2003). The sum of values at the left side of Eq. (4) is often treated as available energy (AE) for the two turbulent fluxes at the right side: sensible heat flux H and latent heat flux L.ET. L is the heat of vaporization (appr. 2.5 MJ kg^{-1}). However, uncertainties arise from heterogeneity in canopy structure or terrain (limited fetch) or by periods of insufficient turbulence (Falge et al., 2001). Also, the sum of the turbulent fluxes often does not match the available energy, which is called the energy balance closure gap (Foken, 2008; Panin and Bernhofer, 2008). Therefore, evapotranspiration from EC is smaller than the ‘true’ ET. After correcting for energy balance closure (Mauder et al., 2020) and proper gap filling (Reichstein et al., 2005), uncertainties are considered stochastic in nature and within the range of 10 % of the available energy.

However, an additional systematic underestimation of ET is associated to rain interception, which is especially relevant in evergreen (coniferous) forests (Van Dijk et al., 2015). Measurements during and after rainfall might show a systematic underestimation of ET, when the canopy and the instruments are both wet and the sensible flux is directed downward. In this case, both turbulent fluxes have different signs and the standard closure correction scheme is bound to fail. At least in cases of low net radiation, as in fall and winter, this leads to a systematic underestimation. An additional sizeable correction of annual ET from eddy-covariance might occur primarily for the spruce site (Fischer et al., 2022). As catchment ET could be used as ‘true ET’, a comparison to ET_{EC} should consider this potential systematic difference.

2.3.3. Water budget related indicators

As an indicator of the evaporative demand of the atmosphere, we used the grass reference evapotranspiration (E_0) of the Food and Agricultural Organization FAO (Allen et al., 1994). It utilises the Penman-Monteith equation and is a common tool to estimate water demand of crops via scaling E_0 by crop coefficients.

The climatic water balance (CWB) is often used as an indicator for the availability of water for runoff and infiltration. CWB is defined as the difference between corrected P and E_0, here. Alternative definitions exist, e.g., P relative to E_0. However, the bias between the two approaches is small. CWB is often used as drought or wetness indicator because it is related to the soil water status and therefore a well-accepted indicator for the growing conditions of crops and forests.

2.3.4. Statistical tools

Main meteorological (T, P, RG, RH and WS) and hydrological variables (R) and derived variables such as E_0 and CWB are considered for the climatological and eco-hydrological analysis. The analysis is based on process understanding in climatology, hydrology and ecology and is performed applying statistics mostly provided in ‘R’ language packages. As a commonly used check on long-term variations, linear trends of yearly sums or averages are tested for significance applying the Mann-Kendall trend test (Kendall, 1955; Mann, 1945) after the necessary check for autocorrelation. A block bootstrapping has to be applied in case autocorrelation exists. In this study, no significant autocorrelation was found. We term trends with a calculated p-value of $p < 0.1$ a “tendency”. P-values of $p<=0.05$ are termed as “(significant) trend”.

In a linear regression model, it is assumed - besides linearity - that the relationship does not change over time. An approach to check the latter assumption is to test the cumulative sum of the Ordinary Least Square residues, which was developed by Ploberger and Krämer (1992). The so called OLS-CUSUM test (and others) was implemented in the R-package “*strucchange*” (Zeileis et al., 2002). Linear and alternative thresholds levels (depending on chosen significance level) are derived from the test

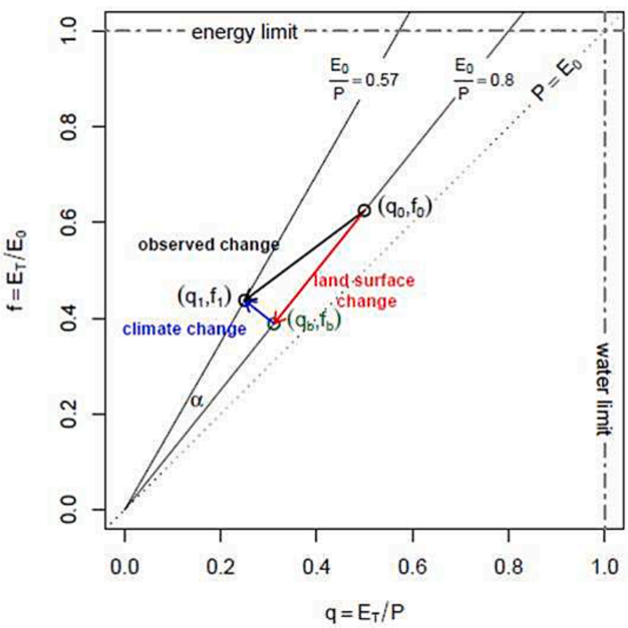

Fig. 3. Energy-water partitioning diagram (Renner et al., 2014, modified). Pure land surface changes develop along the axis (0, 0) and (q_0, f_0) (red line), which can be interpreted as an aridity index. Perpendicular to above axis, climate changes develop (blue arrow). An observed change, e.g., from (q_0, f_0) to (q_1, f_1)), carries mostly the signals of both factors. (For interpretation of the references to colour in this figure legend, the reader is referred to the web version of this article.)

statistic, whereby the alternative threshold is more appropriate, if structural breaks are suspected at the beginning or the end of the time series. An indication of a significant deviation from stationarity is the crossing of the CUSUM estimate with the threshold. CUSUM is a standardised, dimensionless quantity and is interpreted as follows: A CUSUM line fluctuating around 0, would imply a temporal stationary process. Segments with upward slopes indicate above average conditions, while downward slopes indicate below average conditions. Smooth or abrupt peaks indicate the time of a change in the mean. Due to the standardisation, magnitude and time of changes are comparable between different series. The shape of the CUSUM line is not sensitive to the selected time interval, which allows for robust structural change testing.

2.3.5. Budyko framework to separate effects of climate and land use on ET

An attribution of changes in ET to changes in land use and climate is performed according to Renner et al. (2014). The approach is based on Budyko (1974) and Tomer and Schilling (2009) and allows to disentangle climate change effects on the catchment water balance from land use effects. From the long-term water balance, ET can be derived as the difference between P and R. Water storage can generally be ignored for long-term considerations. Under the assumption that the available energy can be described by potential evapotranspiration (E_0), E_0 composes the energy limit for ET. The diagram in Fig. 3 (from Renner et al., 2014) describes two dimensionless measures: water partitioning as $q = ET/P$ and energy partitioning $f = ET/E_0$. The line from the origin of the coordinate system through a point (e.g., q_0, f_0) can be interpreted as an aridity index for the specific catchment. A more humid catchment would lie on a line more to the left. An ET change caused by a pure land surface change manifests through a change of the position along the specific aridity line. Contrarily, a change in the aridity index, i.e., the climatic conditions, manifests through perpendicular deviations from this line. For example, a climatic change towards more humid conditions would increase relative energy partitioning f while decreasing the relative water partitioning q. An observed change in ET (from point q_0, f_0 to point q_1, f_1) can henceforth be separated into a land surface change part

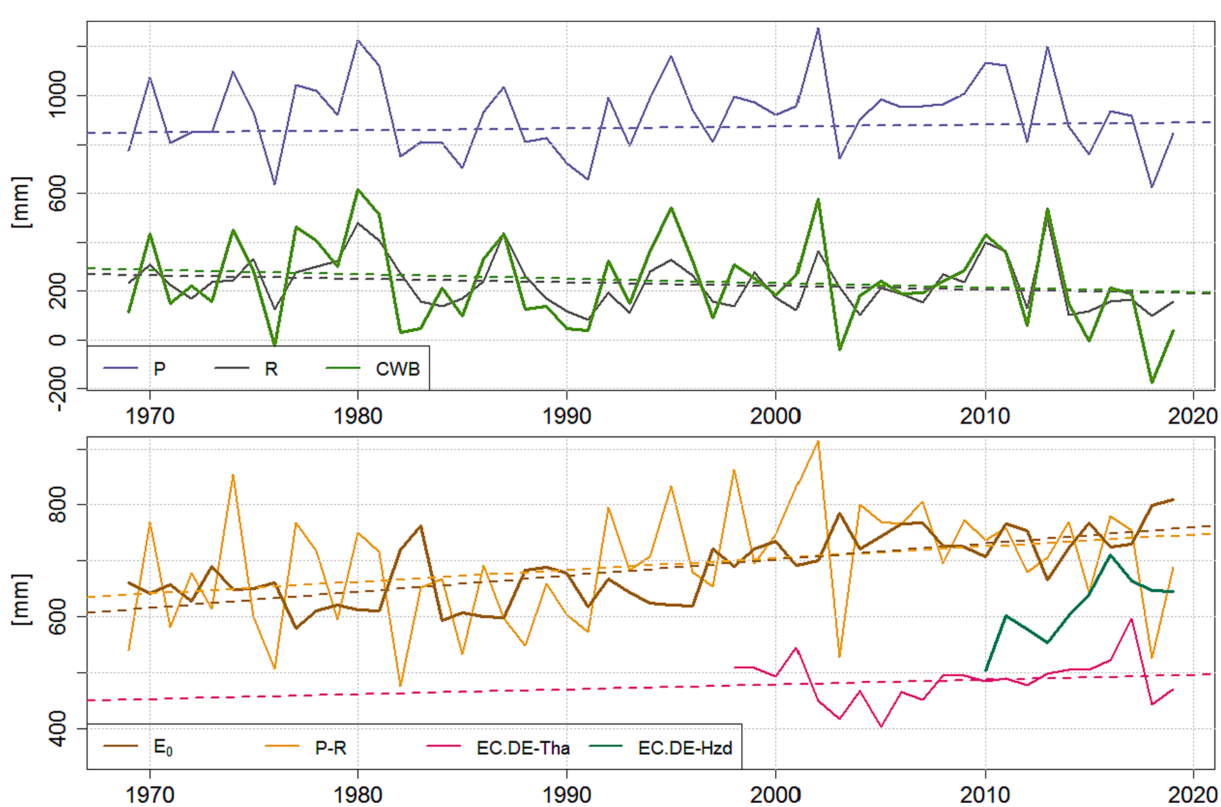

Fig. 4. Yearly values and linear trends of precipitation P, runoff R, climatic water balance CWB, reference evapotranspiration E_0, P-R for WB and ET from EC observations at the two flux towers DE-Tha and DE-Hzd for hydrological years.

Table 2
Climatological values of important climate elements (precipitation is corrected for losses), runoff and evapotranspiration for hydrological years for WB, WA, GB and the EC station DE-Tha. Absolute decadal trend and two-sided p-value are shown for the period 1969–2019.

	Global radiation [W/m^2]	Mean air temperature [°C]		E_0 [mm/yr]	Precipitation [mm/yr]		Runoff [mm/yr]	P-R [mm/yr]	ET_{EC}[*1] [mm/yr]
Station / Period	DE-Tha	GB	WA	GB	WB	WA	WB	WB	DE-Tha
1969–1990	117	7.2	7.7	644	898	916	256	642	
1991–2019	126	8.2	8.7	705	938	934	209	730	
1997–2019	130	8.4	8.9	713	942	935	208	734	479
Absolute decadal trend and p-value	+3.6 W/m^2 $p < 0.01$	+0.4 K $p < 0.01$	+0.4 K $p < 0.01$	+25 mm $p < 0.01$	+41 mm $p = 0.65$	+4 mm $p = 0.78$	−15 mm $p = 0.06$	+21 mm $p = 0.04$	+12 mm $p = 0.53$

[*1] Closure gap corrected ET measurements with EC at DE-Tha; trend calculations are limited to the period 1997–2019.

Table 3
Main hydrological characteristics of WB for the period 1968–2019.

Lowest discharge ever recorded	Mean annual minimum discharge	Mean discharge	Mean annual peak discharge	Highest known discharge
0.1 l/s 17 August 2018	1.9 l/s	33.3 l/s	688.7 l/s	8000 l/s (estimated) 12 August 2002

($\Delta ET_L = ET_b - ET_0$, red arrow in Fig. 3) and a climate change part ($\Delta ET_C = ET_1 - ET_b$, blue arrow). Following Renner et al. (2014) ET_b can be approximated by

$$ET_b = P_0\left(f_0 f_1\, q_0 + q_0^2\, q_1\right) / \left(f_0^2 + q_0^2\right)$$

We also used the Normalized Difference Vegetation Index (NDVI) from the two MODIS (Moderate Resolution Imaging Spectroradiometer) Instruments to estimate the vegetation status independently within the area of WB and the flux towers. The launch of the satellites 20 years ago limits the study period to 2002–2019. The data of the product MYD13A3 Version 6 are provided monthly at 1 km spatial resolution by NASA's Earth Observing System Data and Information System (https://lpdaac.usgs.gov/). Monthly values of nine grid cells centred over the investigation area were used. We used the median NDVI value of the months in the main growing period (May till August) for further analysis.

3. Results

3.1. Time series analysis

3.1.1. Dynamics of hydro-climatological variables

For a first climatological characterisation of WB and the flux towers, means of three periods are shown in Table 2: 1969–1990, representing almost the reference climate without climate change, 1991–2019, the first almost 30 yr. period with greenhouse gas related increase in temperature (+1K), and 1997–2019, the period of parallel measurements at WB and DE-Tha. Time series are visualized along with their linear trends in Fig. 4. All data refer to hydrological years (November to October). We start with the atmospheric control of ET (radiation, temperature, and wind speed) and continue with precipitation, runoff, and ET at catchment level and for the flux tower footprints.

Global radiation shows a significant positive trend over the 50 years. Looking deeper, a declining tendency until the 1980 s followed by a significant increasing trend becomes visible. This is similar to global dimming and brightening (Wild, 2005), however, it is somewhat postponed by at least a decade compared to data from Western Europe. A related change in temperature might exist, but global warming and this regional effect are hard to separate.

The mean annual temperature from Grillenburg has a significant positive trend of 0.4 °C per decade. Mean temperature was 7.2 °C in the period 1968–1990 and 8.2 °C in 1991–2019. The increases occur in all seasons but are most pronounced in summer months.

The mean annual wind speed at 42 m at the forest site (vegetation height changed from approx. 24 m in 1970 to approximately 31 m in 2018) was 3.9 m/s. No additional statistic is given, because the time-series is not homogeneous, as until 1990 data from a no-longer-existing smaller tower had to be used.

The precipitation totals are very similar for the six stations in WB and for the station at WA, according to the analysis of the overlapping period from May 1980 until August 2010. Maximum differences between the stations in WB are mostly around 10 mm but can reach up to 70 mm for single months. However, these differences are not significant and therefore primarily of random nature. A slight altitudinal gradient in mean monthly precipitation sums exists with highest values at the upper stations N1 and N2 (79 mm) and the lowest value at the northerly situated, lower station N4 (72 mm). This gradient of about 105 mm per 100 m height increment is more than the average for Saxony (about 70 mm per 100 m; Bernhofer et al., 2008). The mean monthly catchment average of WB is 77 mm, identical to WA, which is part of DE-Tha. Yearly precipitation sums slightly increased from 898 mm in 1969–1990 to 938 mm in 1991–2019 (not significant), whereby increases occurred in winter months and in July. Until 2017 the precipitation increase was larger; recent dry years reduced it again.

Runoff decreased tendentially between the periods 1969–1990 and 1991–2019 by about 18 % or 50 mm/yr. Within the year, runoff was largest in March and April and lowest in September for 1968–1990 (not shown here). In the period 1991–2019, winter runoff increased due to increased precipitation and due to a decreasing contribution of snowfall and snowmelt. A runoff peak in March and lower runoff in all successive months are contributing to a consistent picture with earlier snowmelt and may be an increase in ET.

The main hydrological characteristic numbers (in German: *Hydrologische Hauptzahlen*) of WB for the period 1968–2019 (Table 3) illustrate the broad range of runoff conditions, especially occurring in recent years: from minimum runoff of 0.1 l/s in 2018 to maximum runoff of around 8000 l/s during the most severe flood in 2002. From analysis of the hydrographs (Schwarze, 2002) runoff components had been separated. Direct flow has a high share of total runoff (54 %), fast base flow (from infiltration areas) is 35 %, and slow base flow plays a minor role (11 %). Isotope measurements proved that a large part of direct flow is water from the time before the flood event. The water has a mean transit time of 38 years (ranging between 8 and 650 years) (Schwarze, 2002).

The catchment ET estimate P-R increased significantly (Fig. 4). This is in accordance with significant trends of grass reference evapotranspiration E_0 as well as of temperature and of global radiation over the complete period of 51 years. However, the closure gap corrected EC data of ET at the tower DE-Tha increased only slightly and statistically not significant. For a broader picture, ETs from both flux towers are included in Fig. 4. While values of DE-Tha are consistently lower than their catchment equivalents P-R by about 250 mm, DE-Hzd seems to catch up

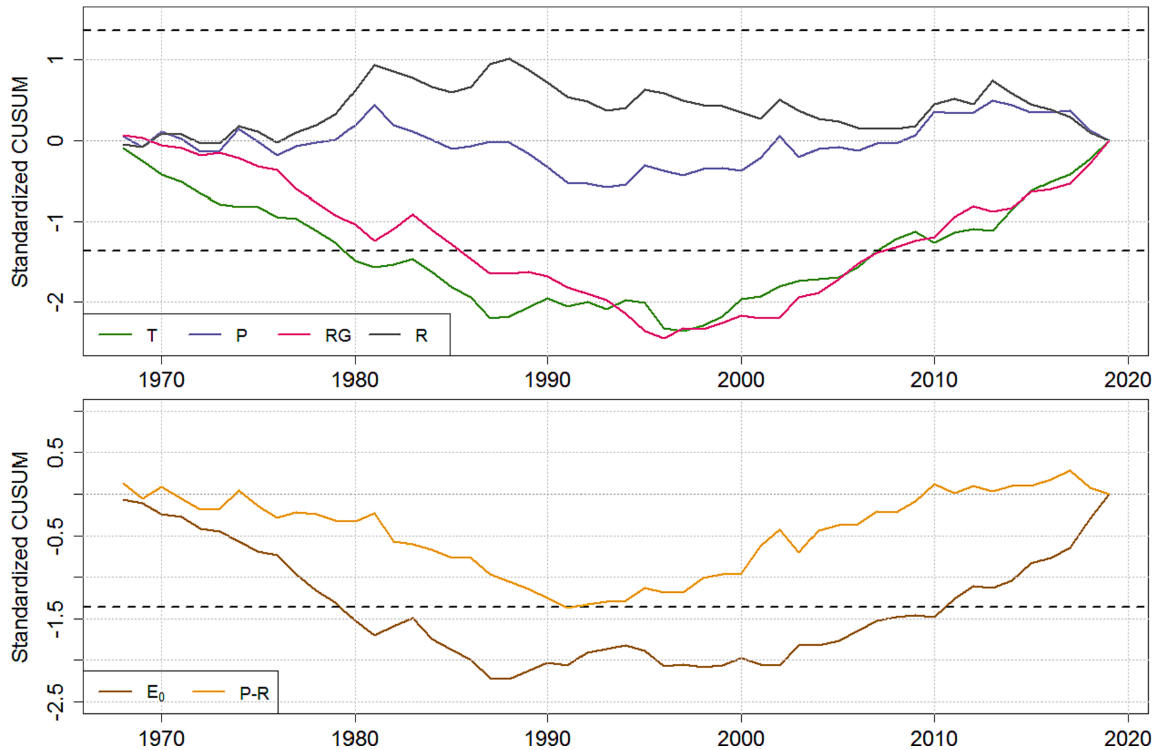

Fig. 5. Results of the CUSUM analysis. Upper panel: Analysis of temperature T, precipitation P, global radiation RG and runoff R. The dashed horizontal line represents the standard boundary for detection of significant changes. Lower panel: Analysis of reference evapotranspiration E_0 and P-R in WB.

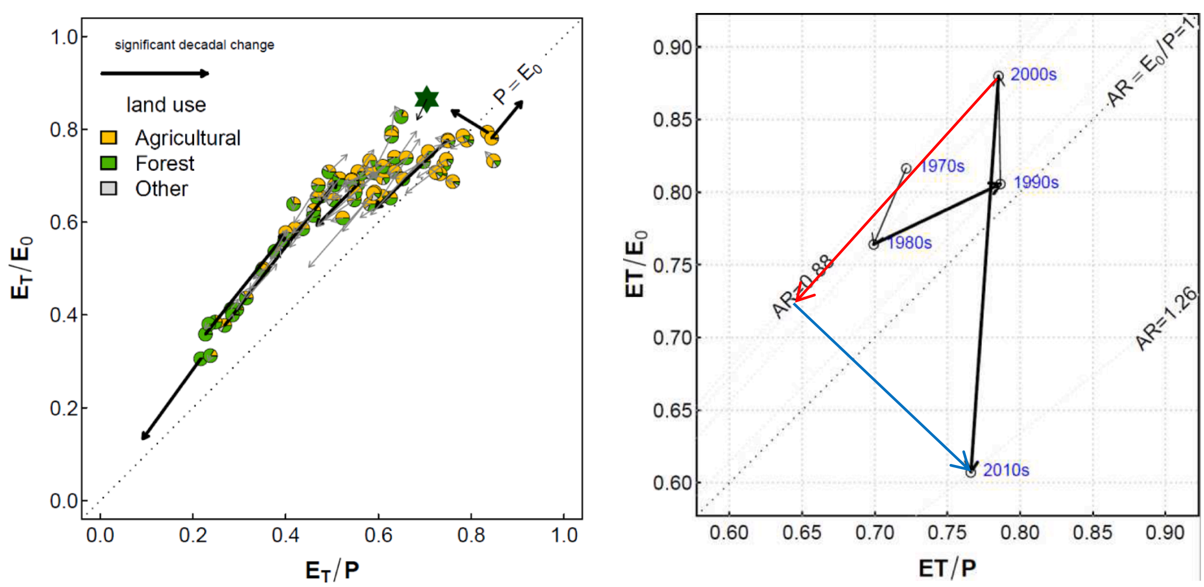

Fig. 6. Left panel: figure from (Renner et al., 2014) plus the green star for WB for the change from 1970 to 1979 to 1980–1989. Right panel: all further decadal changes from 1970 until 2019 for WB. P-R is used as an estimate for ET here. The red arrow illustrates the contribution of land cover changes to observed ET changes from the 2000 s to the 2010 s, and the blue arrow the contribution of climatic changes. (For interpretation of the references to colour in this figure legend, the reader is referred to the web version of this article.)

with P-R around 2014, when canopy closure was reached.

Single annual values of P-R cannot be interpreted directly, but they would have to be corrected with annual water storage change to reproduce actual ET. This can be illustrated by two examples: In the very wet year 2002, P-R is 200 mm higher than E_0. And in the very dry year 2003, P-R is far below E_0. In reality, a large portion of P contributed to storages in 2002 and supported sustained ET in dry 2003. We selected an accumulation time of five years as a compromise between largely reduced bias and sample size of the five years periods. Long-term ET from P-R estimations are very close to E_0 (Table 2). However, grass reference E_0 is reflecting well-watered short grass and is not representing the maximum ET of a forest stand, which might allow even higher rates of ET.

Fig. 4 includes CWB, which is close to observed runoff R. Wet years (1980, 1995 and 2002) result in higher and dry years (1976, 2003 and 2018) in lower CWB than observed R due to storage effects dampening

Table 4
Decadal values of P, RG/L, R, E_0, ET (in mm/yr or °C for T) and corresponding absolute and relative changes between decades as well as the ratios ET/E_0 and ET/P.

Decade	P	ΔP	RG/L	ΔRG/L	T	ΔT	R	ΔR	E_0	ΔE_0	ET	ΔET	ET/E_0	ET/P
1960 s	798		1307		7.1				707					
1970 s	877	80 (10 %)	1274	−33 (-3%)	7.3	0.2	260		686	−1 (-3%)	618		0.90	0.70
1980 s	855	−22 (-3%)	1274	0 (0 %)	7.5	0.2	271	11 (4 %)	693	7 (1 %)	584	−33 (-5%)	0.84	0.68
1990 s	838	−17 (-2%)	1346	72 (6 %)	7.9	0.4	192	−79 (-29 %)	742	49 (7 %)	646	62 (11 %)	0.87	0.77
2000 s	918	80 (10 %)	1389	44 (3 %)	8.4	0.5	208	16 (9 %)	747	6 (1 %)	709	63 (10 %)	0.95	077
2010 s	866	−52 (−6%)	1622	232 (17 %)	8.6	0.2	214	5 (3 %)	937	190 (25 %)	652	−57 (-8%)	0.70	0.75

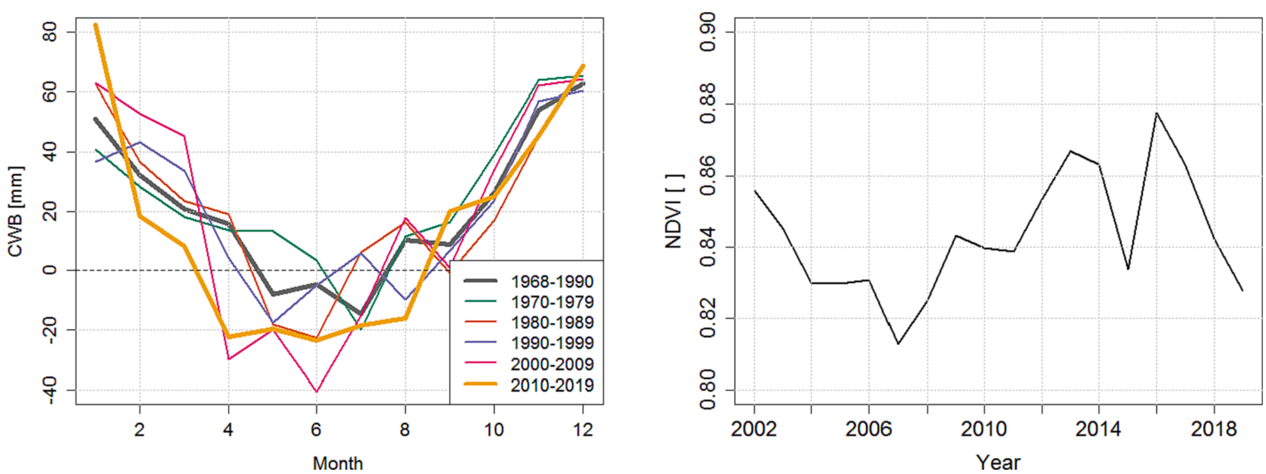

Fig. 7. Left panel: Annual course of the decadal climatic water balance (P-E_0) for WB. Right panel: Maximum summer (MJJA) NDVI at WB.

the catchment response. Precipitation is contributing to storage in wet years, less is converted to R (and vice versa for dry years).

The CUSUM analysis allows detecting structural changes in time. Significant changes are indicated if the curve crosses the horizontal line in Fig. 5. The alternative thresholds levels (mentioned in chapter 2.3.4) form an eclipse. They were omitted in the graph for the sake of clarity, as here they provide no additional information compared to the linear threshold. The P CUSUM series does not show a significant structural change, but rather below average conditions in the early 1990 s, then above average conditions until 2013 and finally a shift towards the dry years of 2018 and 2019. Note that the graph in this analysis will always return to zero by the end of the period analysed. T and RG series show significant structural changes: below average conditions until 1990 s and above average conditions beginning in the late 1990 s. This pattern of RG is typical for the regional effects of air pollution and resulting aerosols (see “Black Triangle” in the chapter 1). T change shows the often-observed breakpoint around 1988 (Renner and Bernhofer, 2011) associated with global warming due to the global increase of greenhouse gas concentrations, and possibly the independent regional effect of changing aerosol concentration. The CUSUM curve of R is very similar to P and is also not significant.

The CUSUM curve of E_0 (lower panel of Fig. 5) shows a very significant breakpoint and reflects the structural changes of T and RG (input data for E_0). This change of E_0 might be more drastic than elsewhere as the global and the regional forcing are in line. The structural change of P-R (actual ET of the catchment including water storage changes) is also significant, despite the complex interplay between the strongly changing driving forces (T and RG) and the hydrologic response of the catchment (R), which also reflects storage and land use. So, climate change alone does not fully explain the observed changes in P-R.

3.1.2. *Analysis of ET changes to separate effects of climate and land use*

Renner et al. (2014) applied a Budyko framework on 68 catchments in Saxony, Germany to determine the relative share of long-term changes of climate change and land-management on ET (here quantified as P-R). For this study the WB was added (green star in Fig. 6, left panel). The points and the star show the mean conditions of the decade 1970–1979, and the arrows indicate the changes to the average value of the next decade 1980–1989. Most forested catchments in Fig. 6 show the effect of increasing sulphur dioxide emissions until 1990 which led to forest die-back in elevated regions of Saxony. Consequences were decreasing ET between the 1960 s and the 1990 s, whereby WB shows a similar tendency (not significant). The influence of other factors determining the water balance like forest management (e.g., more frequent clear-cuts until 1990/ 1992) and well operating drainage channels cannot be excluded. Only minor or no changes occurred in non-forested basins.

The right panel of Fig. 6 zooms into the diagram (ET/P and ET/E_O for the range 0.6–0.9) to facilitate an analysis of WB. It shows decadal changes, whereby the centre of the decade is labelled. Besides the visualization of ET changes in Fig. 6, absolute values and changes in percent relative to the previous period are given in Table 4.

There are always contributions of both land use and climate. The reduction of ET from the 1970 s to the 1980 s is more influenced by the land use or surface effects, which is recognizable by the direction of the arrow, namely mainly along the aridity index. The reason for the reduction of ET is not completely clear. But air pollution (from local sources) and resulting damage of the forest or forest management (clear-cuts, drainage) may play a role. The change from the 1980 s to the 1990 s shows an increase in ET, both surface effects and climate change are relevant. The change towards the 2000 s is characterized by a continued

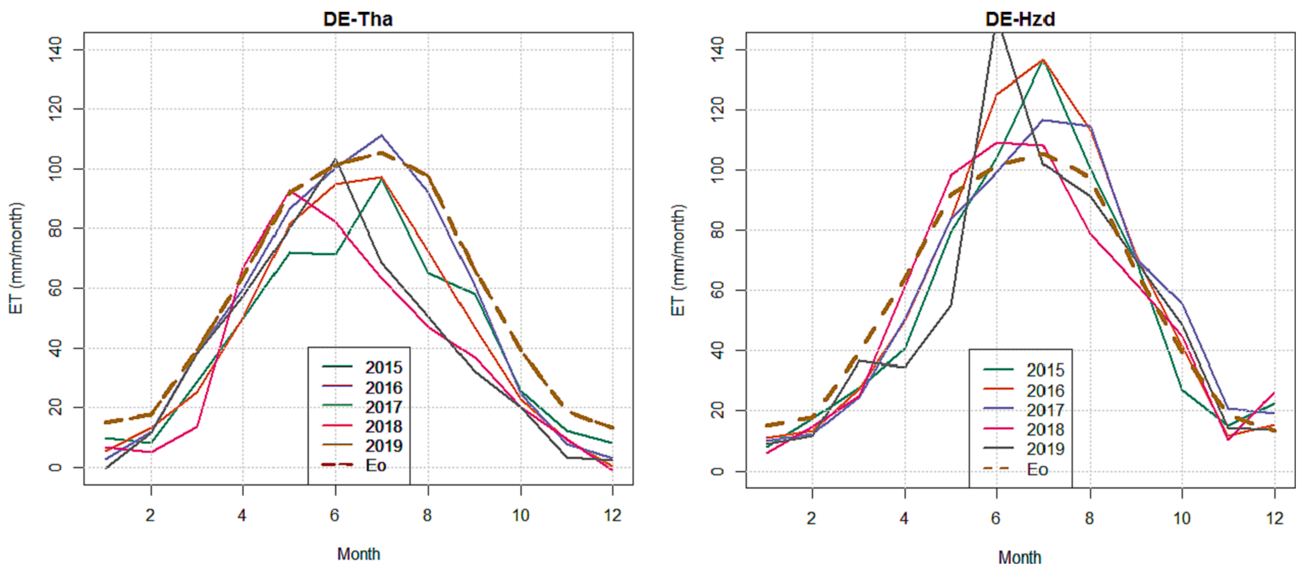

Fig. 8. Comparison of annual cycles of ET for the period 2015–2019. ET was directly measured with EC at DE-Tha (left) and at DE-Hzd (right). E_0 – averaged over the period – was added as dashed line.

increase of ET (10 %), which is related to an increase in precipitation by 10 % resulting in the wettest decade of the 50-year sample. Energy availability increased by only 1 %, henceforth, the ratio ET/E_0 rose considerably. The framework suggests an increased vitality of the forest despite the disturbance due to the cyclone 'Kyrill', which caused significant windbreaks and needle losses in January 2007 (Spank 2010). The following vegetation period showed a minimum in NDVI as demonstrated by MODIS data for WB (Fig. 7). Nevertheless, the forest was able to convert the increase in P into high ET rates.

A pronounced change occurred from the 2000 s to the 2010 s. A large increase in RG (17 %) and in T (0.2 K) led to a strong increase in E_0 (25 %), while precipitation decreased compared to the 2000 s.The aridity index (E_0/P) shifted from 0.8 to more than 1, indicating "semi-arid" conditions in the last decade. The CWB (P-E_0) shows a pronounced water deficit in the growing period (April to August) in the last decade (Fig. 7). A summer water scarcity per se is normal but this severe deficit is unprecedented in the 50-year record. Without water stress, the increase in E_0 of 190 mm/yr should lead to a similar increase in ET. However, we find that ET decreased by 57 mm/yr (-8%). Looking at the Budyko framework in Fig. 6, we see a pronounced drop of the normalized ratio ET/E_0, while the ratio of ET/P remained almost constant, since both ET and P decreased similarly. Hence, climatic conditions and land use change appear to be equally contributing to that change (visualized by the red and blue arrow in Fig. 6). However, the vegetation changes were also related to meteorological conditions! In this decade, there was no drastic change in forest management (excluding potentially still effective consequences of the no longer serviced drainage system), but a series of disturbances affected the forest: windstorms with windbreaks and needle losses in October 2017 ('Herwart') and January 2018 ('Friederike)' followed by strong summer droughts and insect infestations (bark beetle, *Ips typographus*) in 2018 and 2019 as well as damage due to snow load in January 2019 ('Benjamin'). The low NDVI in 2018 and 2019 reflect the impact of these events on the forest stands in the area (Fig. 7).

3.2. Comparing ET from catchment and flux towers

One of our objectives was to clarify whether ET measurements at DE-Tha are representative for WB. While earlier studies show a good resemblance (Frühauf et al., 1999), this study shows a remarkable and persistent difference of around 250 mm/yr (Fig. 4 and Table 2), despite of the practically identical climate and similar land cover. The tower within WB (DE-Hzd) had similarly low ET values as DE-Tha in the first years, but annual values increased until the oak stand reached its canopy closure and showed ET values in the same range as the catchment ET by 2014. Fig. 8 compares seasonal ET variations measured at both EC towers in the period 2015–2019. ET at both EC sites is quite similar in winter and spring. Normally, there is no water limitation because soil water storages are high or even saturated after snowmelt in winter. The ET increase in spring slows down at DE-Tha and reaches its peak in June or July (between 90 and 110 mm/month), whereas the ET maximum at DE-Hzd is between 110 and 140 mm/month in July. Noteworthy is the persistently high evaporation until October at DE-Hzd, which is due to the larger water storage capacity of the soil. In the very dry years 2018 and 2019, the summer maximum is reached one or two months earlier. This is more pronounced at DE-Tha and can be explained with soil and forest stand characteristics (see Appendix A). At DE-Tha, winter losses by interception are higher (evergreen forest) compared to the deciduous forests at DE-Hzd. Combined with the limited soil water storage at DE-Tha this leads to an earlier transpiration reduction at DE-Tha in dry years. Although the record of DE-Hzd is still too short for a final judgement, ET of this flux tower is closer to ET from WB, at least for the most recent and unusually dry years. Potential reasons for the higher ET are soil characteristics, smaller interception losses and different stomatal regulation.

Measurements of the soil water content (not shown here) at DE-Tha show a much earlier drop in dry years than in wet years, reflecting the limited soil water storage capacity. Thus, the difference in ET between the two flux towers is probably larger in dry years than in wetter years.

3.3. Storage analysis

To gain a deeper insight into dynamics of the water balance elements of WB especially during dry years, a water storage analysis similar to Teuling et al. (2013) was performed. But, instead of using ET of DE-Tha for the catchment, we apply a simple approach to obtain plausible monthly ET values for WB. We assume that a) the intra-annual variation of ET in WB can be derived from EC measurements, allowing us to scale ET from EC towers to fit the long-term P-R, and b) that the main reason responsible for ET differences of the two sites – besides methodological uncertainties - are their soil characteristics (discussion in chapter 4.2). Therefore, the oak-regrowth site at DE-Hzd with its similar soil can potentially serve as reference for WB. A simple two-step approach is proposed: (1) The annual difference between catchment ET (including storage change) and ET_{EC} at DE-Tha (excluding storage change) is added

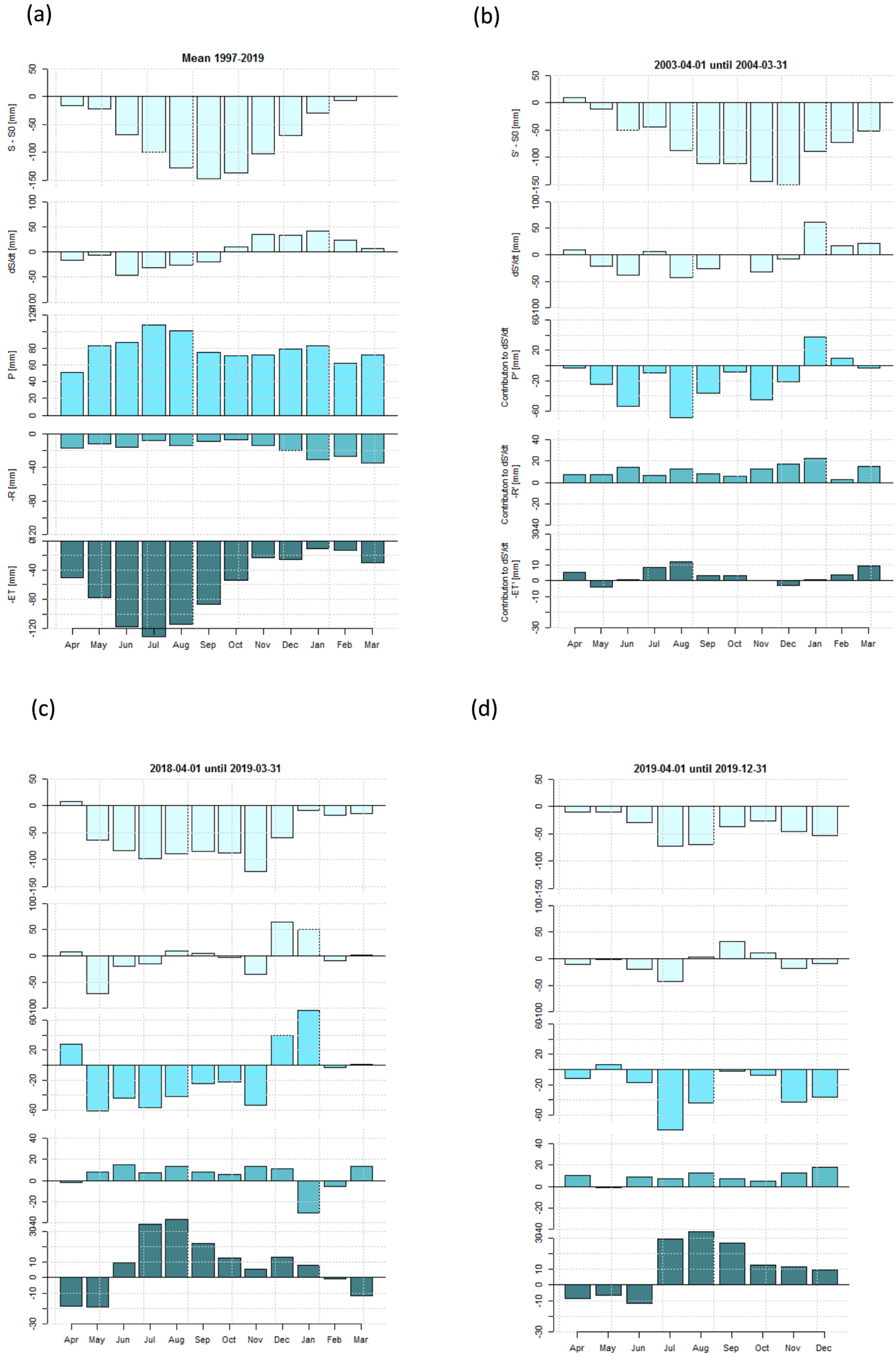

Fig. 9. Long-term means of water budget components in WB (a), and anomalies for single dry years, 2003 (b), 2018 (c) and 2019 (d). Analysis performed for water balance years, i.e., from April till March of the following year. In each panel, plots from above to below show cumulative water storage evolution, water storage, precipitation, runoff and evapotranspiration, respectively.

Table 5
Sum of mean fluxes and anomalies during dry conditions for the summer half year (April-September).

Water balance component	Climatology 1997–2019 [mm/SHY]	Anomaly 2003 [mm/SHY]	Anomaly 2018 [mm/SHY]	Anomaly 2019 [mm/SHY]
dS	−148	−112	−84	−37
P	504	−196	−200	−146
R	75	−57	−50	−45
ET	577	−27	−67	−64

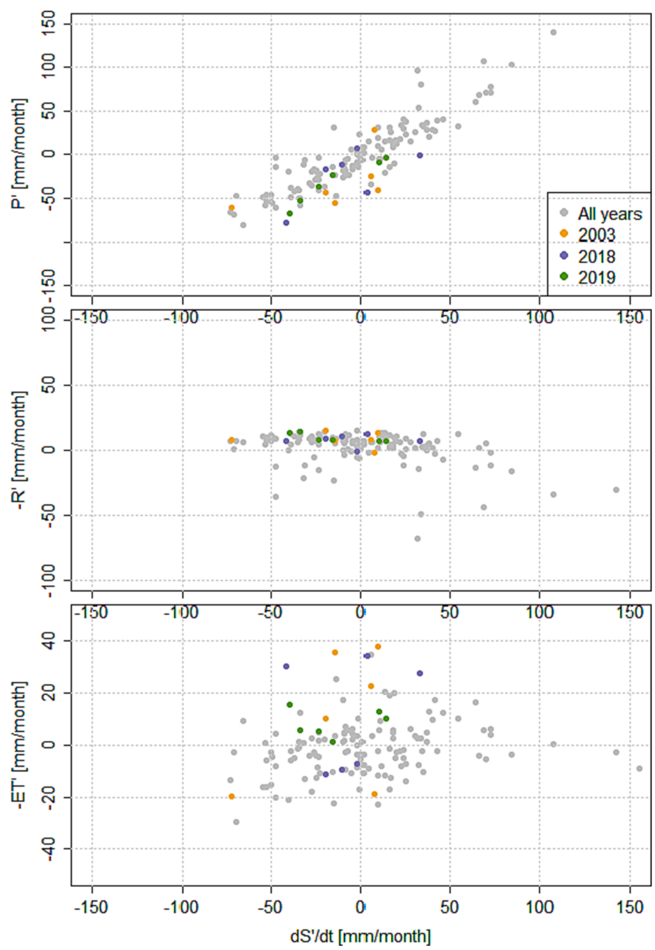

Fig. 10. Contribution of precipitation P, runoff R and evapotranspiration ET anomalies to water storage dS anomaly for all months in the summer half year of 1997–2019. The months of the three dry years are highlighted. This is an update of Fig. 4 in Teuling et al. (2013), whereby corrected ET values were use here.

to the values of ET_{EC}. As the difference became smaller over the years, mean annual differences for 5-year intervals were calculated and added. (2) For a monthly partitioning of the added part, weighting factors were determined that assure a congruence to DE-Hzd for the period 2015–2019. The 12 weighting factors are 0.02, 0.02, 0.01, 0.01, 0.02, 0.15, 0.19, 0.17, 0.16, 0.12, 0.05 and 0.08. Large factors from June until October assure that largest corrections are imprinted during summer and fall months, according to the findings from Fig. 8.

The corrected monthly ET for WB is now used for the storage analysis. Long-term averages of the water balance components of the period 1997–2019 are visualized in Fig. 9a. The graph is designed in such a way that bars above the x-axis contribute to a storage increase and below the x-axis to a storage decrease (note negative signs of R and ET!). For example, high P sums in July (which increase the storage) face even higher ET sums plus small R sums (which reduce the storage). The analysis is performed for water balance years, starting in April assuming that soil is at its field capacity, because of low ET rates in winter and early spring and completed snow-melt in early spring. A typical seasonal cycle manifests with highest P and ET in summer, highest R in winter/early spring and highest dS in winter. Cycles are clearly influenced by ET: beginning with April, ET rates increase strongly until July. Sums exceed precipitation causing a depletion of storage dS and low R values. With the decline of ET in autumn, R increases and dS fills up again. The uppermost plot shows the cumulative storage evolution throughout the year: build-up of a storage deficit until September followed by a stepwise reduction of the deficit until March.

Three dry years (2003, 2018 and 2019) were analysed using monthly anomalies, which were calculated referring to long-term averages (Fig. 9b, c and d). The design of the graphs is similar. 2003 is characterized by severe negative P anomalies from April to December, causing negative R and ET anomalies nearly throughout the whole year (Fig. 9b). A relief from the tense storage situation in January 2004 was not only caused by a P surplus (+38 mm), but also from reduced R (–22 mm) and ET (-1 mm) as a result of depleted soil water (dS = P-R-ET = 38- −22 - −1 = 61 mm).

The water balance year 2018 started with a P surplus followed by negative anomalies until November (Fig. 9c). Negative R anomalies started in May and lasted until December. ET showed positive anomalies until May, as RG and T were high due to a persistent anticyclone over central Europe. Later on, increasing soil water deficit led to a drastic drop in ET until January. The storage deficit continued throughout the year and was reduced somewhat due to a P surplus in December and January. Please note, in this analysis the deficit is not transferred to the next year.

The characteristics of 2019 were very similar to 2018: warm, sunny and a (less pronounced) negative P anomaly. Thus, ET was higher than usual in the first three months. Beginning with July, ET was below average and accompanied by very low soil moisture. R was extremely low throughout the year, and again led to a large storage deficit in December.

The sums of the anomalies accumulated over the summer half year (SHY, i.e., April-September) show that water balance components during dry conditions have changed between 2003 and 2019 (Table 5). P anomalies are comparable in 2003 and 2018 (around −200 mm/SHY), leading to an R anomaly of around −50 mm/SHY in both years. But, in 2018 the ET anomaly is much more pronounced than in 2003 (-67 vs −27 mm/SHY). In 2019, this trend continues. Although the P deficit is less (-146 mm/SHY), the R anomaly remains nearly constant (-45 mm/SHY). And interestingly, the ET anomaly is of the same magnitude as in 2018.

To test for the influence of individual water budget components on the water storage, all months of the summer half year of the period 1997–2019 were included (Fig. 10). We found a clear dependency of storage anomalies to P anomalies ($R^2 = 0.74$), while no significant influence of -R or corrected -ET anomalies could be detected ($R^2 = 0.14$ and 0.03, respectively). The thesis of the Teuling et al. (2013) that months with below-average rainfall tend to have above-average ET, which acts to amplify the storage deficit, is not supported by this dataset. The increasing soil water deficit seems rather to reduce ET during summer and fall in WB.

4. Discussion

4.1. Factors contributing to the dynamics of water budget components

The dynamics of the hydro-meteorological variables show the expected combination of climate related forcing during the 50 years of operation, like (i) natural climate variations, (ii) global warming, and (iii) regional climate specifics as exposure to certain weather patterns and effects of local air pollution. Despite this climate signal, land surface

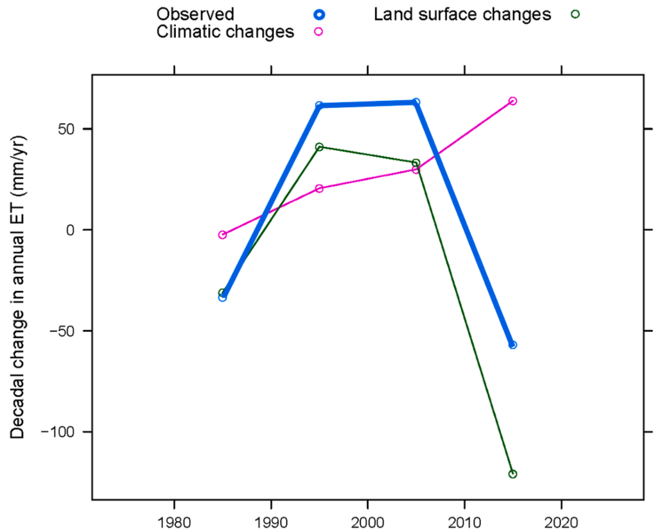

Fig. 11. Land-surface and climate related contributions of the observed ET anomalies (after Renner et al., 2014). The points illustrate the changes from the previous decade. For example, the observed negative change in ET (-40 mm/yr) from the 1970 s to the 1980 s are exclusively caused by land surface changes.

changes were equally important, such as changes due to forest management or forest damages.

The large natural climate variations are most obvious in the P series (Fig. 5), the temporal variability being independent of the long-term trends in T and RG. Global warming relates to a T increase starting around 1988. However, the "regional dimming" between 1960 s and 1990 s and later the "regional brightening" starting in the late 1990 s (similar to global dimming and brightening; Philipona et al., 2009) was a special feature, modulating the global climate signal regionally. Aerosols related to sulphur dioxide emissions from coal burning prolonged the dimming effect until 1997 compared to sites elsewhere in Europe (Jones and Moberg, 2003).

Reference evapotranspiration E_0 resembles the long-term changes of T (and RG). A significant linear trend of E_0 is in line with most catchments of Europe (Teuling et al., 2019). The breakpoint analysis revealed that the significant increase started around 2000. P-R, as an estimate for actual ET of WB, is significantly increasing, linearly, and a significant structural change was identified in early 1990 s. According to Renner and Bernhofer (2011), Saxon catchments above an altitude of 740 m showed a breakpoint in T and in the runoff ratio (R/P) in 1988, probably due to a higher sensitivity of snow-melt driven catchments. This seems to hold also for WB, despite the altitude of only around 400 m.

Catchment response of actual ET to changes in climate or land use may differ in their temporal response. However, both factors contribute to different degrees on a decadal time scale, as the Budyko framework analysis has shown. Interannual variability of P-R reflects (i) the available buffer due to catchment water storage, and (ii) the atmospheric drivers of ET (see Teuling et al. 2013). This favours high ET in dry years, as far as sufficient storage exists. For consecutive dry years, actual ET of the second dry year declines regardless of the high E_0.

4.2. Factors contributing to the lower ET from the EC flux tower

For 1997 to 2019, the catchment ET estimate P-R could be directly compared to the flux tower ET. Generally, the flux tower ET_{EC} variation is low, typically between 450 and 500 mm/yr. Extremes were recorded with 380 mm in 2003 and 600 mm in 2017. The catchment response P-R varies from 430 to 950 mm/yr. No statistical relationship was found between both datasets. In the following we look at possible reasons for the systematic differences between catchment and tower ET, namely differences in climatic conditions, soil, land cover, and its management

Table A6
Land cover of study sites. If not stated otherwise, percentages refer to the catchment WB and the respective footprint of the towers in DE-Tha and DE-Hzd.

Site	Year of Inventory	Norway Spruce *Picea abies*	Scots pine *Pinus sylvestris*	Deciduous [*1]	Age [years]	Method
WB	1988	72 %	12 %	16 %	60	complete forest inventory of over and under storey conducted by the Forestry Office Tharandt
	2005	70 %	12 %	18 %	60	biotope mapping based on airborne colour-infrared orthophotos (Tröger, 2012)
	2013[*2]	70 %	9 %	21 %	63	complete terrestrial inventory of over and under storey conducted by Saxon Forest Agency
DE-Tha	1999	72 %	15 %	13 %	71	random samples of over storey trees of existing forest plots were taken in a radius of 500 m around the tower DE-Tha (Mellmann et al., 2003)
	2013[*2]	75 %	3 %	22 %	75	complete terrestrial inventory of over and under storey conducted by Saxon Forest Agency
	2019	81 %	2 %	17 %	maximal 118 [*3]	complete inventory of the over storey within four plots (25 m diameter) around the tower DE-Tha, supplemented with further exemplary plots in a 500 m diameter (standardized ICOS method, compare Gielen et al., 2018).
DE-Hzd	1988[*4]	85 %	14 %	1 %	–	complete forest inventory of over and under storey conducted by the Forest Agency of Tharandt
	2013[*2]	23 %	0 %	77 %	19	complete terrestrial inventory of over and under storey conducted by Saxon Forest Agency

[*1] Mainly larch (*Larix decidua*), beech (*Fagus sylvatica*), birch (*Betula pendula*) in WB and DE-Tha. Mainly oaks (Quercus robur and Quercus rubra) in DE-Hzd.
[*2] Forest pathways were identified separately and account to 4–5%. These shares were - for the sake of consistency – added to the species according their shares.
[*3] Tree ring analysis of four trees resulted in 114–118 years in September 2020.
[*4] For DE-Hzd no separation between spruce and pine was available. The 99% coniferous forest were divided according to the share in WB in 1988.

Table B7
Metadata of hydro-meteorological stations (WB-Wernersbach, WA-Wildacker, GB-Grillenburg, EC stations DE-Tha and DE-Hzd).

Variable	Stations	Observation period	Temporal resolution	Instrument and site changes
Precipitation [mm]	WB, stations N1-N6	Since 12.1967 N6: 05.1990–08.2010	- Daily - Since 1992 hourly - Since 2002 mostly and since 03.2011 all with 10 min in summer	– 12.1967 Hellmann 200 cm^2 (zinc coated, since December 2002 stainless steel) – 1969/72 additionally, recording rain gauge – 02.1974 wind shield installed for Hellmann – 1995 additionally, tipping rain gage with data logger – 10.2003 additionally, Pluvio (Ott) at N2 - site changes: N1: 05.1972, 10.1987, 05.1999, 10.2010 N2: 05.1972, 10.1988, 05.1994, 05.2008, 11.2012, 04.2016 N3: 01.1972, 09.1983, 01.1994, 05.2008, 04.2016 N4: 05.2010 N5: 06.1986, 04.1990, 05.2008, 01.2015 N6: 04.1997
	WA	Since 01.1968	- Daily - Since 1990 hourly (no snow) - Since 1997 10 min	– 12.1967 Hellmann 200 cm^2 – 1997 additionally, tipping rain gage with data logger – 01.2000 additionally, balance rain gage Pluvio (Ott)
Tmax [°C]	GB WA	Since 12.1967	Daily: - from 9 to 9 pm - since 1984 from 7 to 7 pm	- Maximum thermometer, Pt100, VAISALA HMP 45 - Maximum thermometer
Tmin [°C]	GB WA	Since 12.1967	- since 1998 from 0 to 24 h	- Minimum thermometer, Pt100, VAISALA HMP45 - Minimum thermometer
Tmean [°C]	GB	Since 12.1967	Daily: - mean of 7 am, 9 pm and 2 times 9 pm - since 1984 mean of 1 am, 7 am, 1 pm and 7 pm - since 1998 30 min - since 2005 10 min	- Thermo-Hygrograph, Pt100, VAISALA HMP45
	WA	Since 12.1967	- Until 11.1997 see Tmean for GB - Since 12.1997 30 min - Since 8.2004 1 min	- Thermo-Hygrograph
RH [%]	GB	Since 12.1967	See Tmean	- Psychrometer, Thermo-Hygrograph, dew point sensor, VAISALA HMP45
Wind speed [m/s]	WA	01.1968–01.1997	Daily: mean of 1 am, 7 am, 1 pm and 7 pm	- Anemometer, 19 m, forest clearing
	GB	Since 06.1998	– 30 min - Since 08.2011 10 min	- Cup Anemometer, 12 m, grassland
	DE-Tha	Since 10.1995	– 30 min - Since 03.1997 10 min	- Cup Anemometer (THIES), 42 m, above forest
Global Radiation [W/m^2]	WA	01.1968–12.1996	Daily	- Pyranometer, 20 m, shortwave upper half-space (old wooden tower)
	DE-Tha	10.1995–09.1998 10.1997–06.2012 Since 11.2007	– 30 min - Since 03.1997 10 min	- Pyranometer (LAMBRECHT), 41 m, shortwave upper half-space - Radiation sensor (LAMBRECHT), 37 m, shortwave upper half-space - Radiation sensor (CNR1/CNR4), 37 m, shortwave upper half-space
Water level [cm]	WB	Since 12.1967	- Hourly - Since 02.1992 10 min	- Two level recorders (0 … 40 cm resolution 1:1, >=40 cm resolution 1:5), – 1992, additionally pressure sensor ‚OTT Hydrus'
	Oberer Wernersbach, 1.0 km^2	Since 1992	- Hourly - Since 04.1994 10 min	- Level recorder and, additionally, pressure sensor , OTT Orpheus'
	Triebenbach 1.5 km^2	1992–1998	- Hourly - Since 04.1994 10 min	- Level recorder – 1992, additionally pressure sensor , OTT Orpheus'
	N-Bach 0.58 km^2	1991–1998	- Hourly - Since 04.1994 10 min	- Level recorder and pressure sensor
	Etzenbach 0.21 km^2	1992–1998	- Hourly	- Level recorder
Groundwater level [m]	Three sites Two sites	1974–1998 Since 2010	Occasionally	- Whistle pipe – 2016 submersible probe
Spring runoff, temperature [l/s], [°C]	27 gages	1989–1998	~ Monthly	- Bucket, stop watch and thermometer
Soil moisture [ ]	13 sites in WB, until 150 cm	1970–2000	~ Monthly	– 1970 s and 1980 s with neutron probe – 1989–2000 with neutron probe S-23 (Wittich Labortechnik)
	20 sites at *N*-Bach	1991–2001	10 min	- Tensiometer (SM-Tens, IMKO)
	4 sites at DE-Hzd	Since 05.2009	10 min	-three FDR probes (ML-2x, Delta T) and one TDR probe (SoilVUE 10)
Energy balance and sensible and latent heat fluxes	DE-Tha, experimental tower, 42 m	Since 1996	-Hourly -Since 2016 30 min	– 03.1996 temperature and 3D wind speed with ultrasonic anemometer (USA1 METEK) – 20 Hz – 07.1996 CO_2 and H_2O concentrations with gas analyser (LI-6262,

(*continued on next page*)

Table B7 (*continued*)

Variable	Stations	Observation period	Temporal resolution	Instrument and site changes
				LiCor Inc., Lincoln, NE, USA) and temperature and 3D wind speed with ultrasonic anemometer (GILL SOLENT R2, Gill Instruments Lymington, UK) – 11.2006 GILL SOLENT *R*3 (Gill Instruments Lymington, UK), LI-7000 (LiCor Inc., Lincoln, NE, USA) – 03.2016 additional GILL HS-50 (Gill Instruments Lymington, UK), LI-7200 (LiCor Inc., Lincoln, NE, USA) - soil moisture, soil heat flux, soil temperatures, short and long wave radiation
Energy balance and Eddy Covariance	DE-Hzd	Since 2010	30 min	- temperature and 3D wind speed with ultrasonic anemometer (CSAT3 from Campbell Scientific ltd., Logan, Utah, USA), 10 Hz - CO_2 and H_2O concentrations with open-path infrared gas analyser (LI-7500 from LiCor Inc., Lincoln, NE, USA) - soil moisture, soil heat flux, soil temperatures, short and long wave radiation

as well as at methodological aspects of the two methods to arrive at ET.

4.2.1. Climate and site characteristics

Climatic differences between WB and DE-Tha are small. Precipitation at DE-Tha is 1.3 % higher than at WB. RG will be the same, while slope and aspect will produce small differences in effective net radiation Rn. Wind speed may be a bit lower for WB (Westphal, 2007). Overall, neither of these factors nor their combination explain the observed differences in ET.

The larger area of WB compared to the flux tower footprint, as well as the location of the flux tower (an infiltration site at a small "plateau"; see Fig. 1) lead to higher heterogeneity of WB as well as to some bias in the site characteristics. Along the small tributaries of Wernersbach (*N*-Bach, Etzenbach and Triebenbach), groundwater influenced soils dominate, where a riparian vegetation has prolonged access to water in dry periods. These parts of the catchment will disproportionally contribute to ET.

To address soil characteristics, important data like usable field capacity UFC or skeletal share SKV are listed in Table 1 for WB, DE-Tha and DE-Hzd. Soils in WB and at DE-Hzd are capable to store more water in the soil column than soils at DE-Tha (high usable field capacity) and have henceforth favourable conditions for ET. In other terms, soils at DE-Tha have better infiltration characteristics due to high skeletal fraction and probably due to preferential flow. This is supported by the annual courses of ET_{EC} (Fig. 8), which show significantly lower ET between July and October at DE-Tha compared to DE-Hzd, associated to the limited soil water availability and the tighter control of stomatal opening at the coniferous stand DE-Tha.

Land cover and its management are additional characteristics to be addressed. Both sites, WB and DE-Tha, were covered with 75 % coniferous trees and around 20 % deciduous trees in 2013. The forest stand in the footprint of DE-Tha is about 40 years older and approximately 10 m higher. LAI was estimated to be 5.1 for WB, 5.6 for DE-Hzd (in summer) and 4.9 m^2/m^2 for DE-Tha in 1999 (Wutzler, 2002). Despite lower transpiration rates per LAI of older trees (Köstner, 2001), even the combined effect of age and LAI does not explain the difference in ET of WB and DE-Tha.

4.2.2. Uncertainty and bias of the different methods to derive ET

Finally, we need to address potential systematic differences in the methodologies applied to arrive at ET values. Besides random uncertainties, there are potential systematic effects that deserve attention.

The catchment water balance ("hydrological") approach assumes that the mean water storage of a sufficiently long record becomes small enough to be ignored relative to mean ET. This is only true, when the record is long enough, typically 5 to 20 years, and a few further assumptions are met: (i) the precipitation measurements and their correction, as well as the water level measurements and the rating curve are correct, (ii) the complete runoff is recorded at the catchment outlet including groundwater contribution to R, and (iii) the groundwater related catchment size is the same as the surface related size. Bias in runoff by undetected sub-surface flow can be neglected, as the concrete wall across the valley prevents any bypass at the weir (see chapter 2.2.1). Severe floods and instrument failure of the WB stream gauge need careful correction and gap filling, respectively. In those cases, the missing runoff was added manually after a careful analysis of other gauges and indirect indicators of the water level or via modelling. For the purpose of an uncertainty estimate, let us assume that the uncertainty in R due to (i) and (ii) is small and its systematic effect for an average of 50 years is below 1 %. Finally, the subsurface catchment might be 0.2 km^2 or 4 % (Müller, 1998) or even 0.4 km^2 (8 %, other local experts) smaller than the surface catchment due to the underlying geology. Considering a subsurface catchment with a reduced area of 4.2 km^2 would increase R and henceforth reduce P-R values corresponding to systematically lower ET. To estimate this bias, the following assessment was made. Using the mean contribution of slow groundwater flow of 11 % to R (Schwarze, 2002) and applying the reduced catchment size, the maximum systematic effect of the sub-surface size difference will be around 1 % for R and only −0.3 % relative to ET. Most of the above effects are random for periods of five years or more, besides the small catchment size effects. In summary, while catchment ET has a very low time resolution with little random uncertainties, also the maximum systematic bias of catchment ET is small. The estimate of the potential bias is well below 2 %, explaining only a marginal part of the difference between ET values of WB and DE-Tha.

Uncertainties and bias in ET from micrometeorological measurements via EC originate from general shortcomings of the technique and specifics related to water vapour flux. EC is considered as the state-of-the-art technique to record fluxes from all kind of surfaces with sufficient homogeneity in the footprint. Generally, EC requires turbulent conditions, which are often missing at low wind speeds and stable stratification. Data points (half-hourly fluxes) with insufficient turbulence lead to low values of turbulent heat fluxes detected via EC. EC typically fails to measure 100 % of the fluxes balancing the available energy (net radiation minus soil heat flux minus heat storage change). Some reasons of this closure gap had been identified, but a consistent picture on this important issue is still only emerging (Mauder et al. 2021). Closure gap correction of ET is done based on redistributing according to the Bowen ratio of the uncorrected EC fluxes (see, e.g., Falge et al., 2001; Pastorello et al., 2020). However, Van Dijk et al. (2015) conclude that standard FLUXNET correction approaches need to be reworked for the stable conditions after rainfall. As interception under stable conditions with a negative sensible heat flux is a common process for evergreen needle leaf trees in humid temperate climates (Bernhofer et al., 2003), we expect a considerable ET underestimation at the spruce site DE-Tha. While providing a high temporal resolution, uncertainties in flux tower ET can be quite large and systematic. A more precise estimate of this systematic bias for DE-Tha is subject of the investigation by Fischer et al. (2022), while in the following we continue to evaluate its contribution relative to the observed ET difference. Here, the use of the residual ET according to the energy balance (AE-H)/L cannot serve as an upper limit of ET. For periods of negative H, actual ET can be even larger than the measured residual. Nevertheless, the mean residual ET is about 650 mm and therefore much closer to the catchment ET (compare Table 2).

4.2.3. Quantification of ET differences

As plausibility checks we used interception and transpiration measurements as well as simulations with a hydrological model.

Fortunately, various auxiliary measurements exist at DE-Tha and many studies using data of DE-Tha had been published since the start of the flux measurements in 1996. Recently, 25 years of site water budget measurements were analysed to arrive at interception (Grunicke et al. 2020). They showed a mean annual below-canopy precipitation of around 55 % and henceforth interception “losses” of around 45 % of P for the vegetation period between April and October (1997–2018). Because of a remarkably higher LAI at the location of the below-canopy rainfall measurements compared to the LAI of the flux tower footprint, we applied a scaling factor of 0.8 according to the LAI ratio. This yields an interception of 36 % and a below-canopy precipitation of 64 % of P. Sap-flow measurements at the same site for the period 2001–2007 (Clausnitzer et al., 2011) showed a 55 % contribution of transpiration relative to below-canopy precipitation. Applying these relationships to the period 2006 to 2019 leads to: 583 mm of rainfall, 210 mm of interception and 205 mm of transpiration for the vegetation period. The sum of interception and transpiration of 415 mm is already close to the mean annual tower ET of 497 mm. Any additional ET in the November to March period and the annual sum of soil evaporation is not supported. A conservative estimate soil evaporation and understorey ET is 100 mm for the flux tower site, while additional 30 mm is to be expected from winter transpiration. For interception, especially in the presence of snow, we have no serious estimate, but in mild winters interception might be high. We assume here an interception loss of 24% of winter precipitation (357 mm) which yields 86 mm. Adding up all ET components results in 631 mm/yr, which is 134 mm/yr more than the observed value of 497 mm/yr for DE-Tha in the period 2006 to 2019. Without above mentioned LAI scaling factor (LAI estimates over a longer period of time in larger areas are difficult.) we calculate 179 mm/yr more. Therefore, ET_{EC} at DE-Tha seems systematically too low by about 130 to 180 mm despite its correction for closure of the energy balance.

The water budget model BROOK90 (Federer, 2021) is already widely used (Luong et al., 2021; Schwärzel et al., 2009) to compute water balance components for the Tharandt Forest, with a focus on ET components. A recent study (Vorobevskii et al., 2022) highlights different data environments of BROOK90 (local, regional and global) and the importance of parameterization and forcing. There, DE-Tha was modelled for the period 1997–2020. Three model set ups, which were only parametrized and not calibrated, simulate an ET of around 650 mm/yr (compare Fig. 4 in Vorobevskii et al., 2022). In contrast, the calibrated version (according to ET_{EC}) simulates 480 mm/yr. The uncalibrated models simulate a mean interception of 27 %, whereas the calibrated models of only 8 %. Compared to observations of 39 % for the late 1990 s and 33 % for the 2010 s (Grunicke et al., 2020, scaled as mentioned above), this clearly shows uncertainties in ET partitioning, especially for the calibrated version. We argue that the difference of around 170 mm/yr between calibrated and uncalibrated models is another hint for the significant underestimation of ‘true’ ET by EC measurements at DE-Tha.

Based on the above reasoning, we speculate that the EC flux correction algorithm for the closure gap is insufficient for interception episodes, when negative sensible fluxes boost interception related latent heat flux (Fischer et al., 2022). This process is most obvious for daily totals during late fall and winter with almost zero net radiation. Nevertheless, it is also relevant for short periods after rainfall in spring and summer.

Resuming, when tower ET is corrected for the interception loss in ET_{EC} of about 130–180 mm/yr (rough estimate, for details see Fischer et al., 2022), we arrive at a tower ET value of 630 to 680 mm. The remaining difference of 40 to 85 mm is attributed to site conditions.

4.3. Did ET change due to climate change?

As far as meteorological drivers are concerned, significant positive trends were found for T and RG for the complete period 1968 to 2019, and the CUSUM analysis revealed significant breakpoints around 1988 and 1996, respectively. Global radiation decreased between 1960 s and 1990 s but returned to normal between around 1997 and roughly 2010. These changes led to a significant increase in E_0, which are in line with other sites in Europe (e.g. Teuling et al., 2019) and which was also reported earlier for the trends in T, P, RG, E_0 and ET in the complete Elbe catchment (Teuling et al., 2009).

The catchment ET at WB is significantly increasing, despite the insignificant trends in P and R. The reason cannot be attributed to climate alone, it is rather a combination of changes in forest management (more harvesting before 1992; thereafter managing the pure coniferous stands toward mixed or deciduous stands and by not servicing the drainage system in WB), changes in the vegetation status, and climate change.

By applying the analysis after Renner et al. (2014) for an assessment of the respective contribution of climate change vs land use change for the complete WB dataset until 2019, we could identify various phases in changes of ET (Fig. 11). The transition from the 1970 s to the 1980 s is characterized by a reduction of ET exclusively caused by land surface changes, namely damaged vegetation due to “acid rain”. Climatic contributions are always positive in the next decades due to the combination of global warming and regional “brightening”. From the 1980 s to the 1990 s ET increased significantly besides climatic influence due to healthier forest stands and altered management practices. The step to the 2000 s is characterized by a further small increase in ET, which is mostly due to favourable climatic conditions. The ET change in the last decade, the 2010 s, is extraordinary: despite increasingly favourable climatic conditions, a drastic drop of 57 mm/yr in ET was observed (see Table 4). This decrease can only be explained by a reduction of ET by changes in land-cover since the available energy increased considerably in the last decade. Considering only the direct climatic impacts, ET would have increased according to the attribution method. However, land surface effects more than offset the climatic effects and led to a decline in ET. We presume that climatic variations lead to changes in the land surface reducing actual ET. The dry and hot years 2018 and 2019 caused direct drought damages and allowed an unprecedented bark beetle infestation. Furthermore, heavy wind storm and snow load events damaged the tree crowns practically in all of Saxony (e.g., SMUL, 2019). Thus, these extreme events have lasting effects on “land use”. As their intensity and frequency is probably associated with climate change, they may trigger feedbacks intensifying climate change.

Applying an approach similar to Teuling et al. (2013), an analysis of the dynamics of and the interactions between the water balance components was performed and altered ET characteristics during droughts were identified. Instead of using ET from the EC tower DE-Tha for WB, we derived a more representative ET estimate combining monthly catchment and tower ET. The dry years 2003, 2018 and 2019 were analysed relative to the long-term average. In contrast to findings of Teuling et al. (2013), these extremely dry years did not show above average or average ET. Teuling et al. (2013) stated a “drought paradox” for WB and two other catchments in Europe, which means that P deficits are sometimes accompanied by high ET rates, amplifying water storage anomalies. According to our analysis, this drought paradox was only present at the beginning of the summer in the dry years 2018 and 2019.

Differences between our results and those of Teuling et al. (2013) result from a different data base. Teuling et al. (2013) used ET observations of the EC tower DE-Tha directly until 2011, assuming tower ET to be representative for the catchment Wernersbach (e.g. Frühauf et al., 1999). The current study is based on a combination of tower ET and catchment ET observations until 2019. The systematic underestimation of more than 200 mm/yr at DE-Tha was strongly reduced by combining both data sets. Applying ET from DE-Tha for Wernersbach would result in a long-term water storage of 255 mm/yr for the period 1997–2019 (P-R-ET_{EC} = 942–208-479, see Table 2). The basic assumption of catchment ET is that the difference between precipitation and runoff represents the actual ET for periods long enough to reduce storage variations considerably (small compared to other uncertainties). Then long-term water storage is set to 0 mm/yr.

Considering this difference in long-term storage explains the different results in ET from Teuling et al. (2013) and this study. The general higher level of storage in the work of Teuling et al. (2013) allows higher ET values even during drought events, which contributed to the drought paradox. We think that tower ET is too small (despite the EC closure correction) and the overall ET is somewhat higher in Wernersbach catchment (due to soil characteristics). During long-lasting drought events, the soil water supports ET for some months, later followed by ET reductions. As a consequence, our necessary correction (rescaling) of ET changes the magnitude and sometimes even sign of ET anomalies. Therefore, we arrive at different conclusions concerning ET for typical dry years for the longer data set.

In fact, ET acts as a drought aggravating factor only when enough soil water (and ground water) is available, which is generally the case in spring. In summer, ET is considerably lower than average during drought events. Main driver of the storage dynamics is P. Runoff was reduced to the minimum of groundwater based discharge which is on average 11 % of total R (Schwarze, 2002). With a residence time of 38 years, these runoff components are barely influenced by actual moisture conditions, resulting in a relatively constant flow of “old” ground water. The contribution of ET to storage evolution differs between dry years, as the seasonal rainfall distribution, evaporative demand and antecedent soil moisture conditions differ as well. A common drought pattern was not detected, rather an intensification of ET anomalies becomes apparent (compare Table 5). However, the sample size is too small for a final judgement.

Nevertheless, there is no significant trend in ET_{EC} at DE-Tha. But it is still possible that such tendencies will be found after correcting ET_{EC} for interception effects on EC.

5. Conclusion

Actual evapotranspiration ET, land use, climate and its change are non-linearly coupled, making simple cause-response relationships hard to find. However, there is enough evidence for a set of well supported statements on the water budget of the Tharandt Forest as an example for other (coniferous) forests in a similar climate.

- Long data records are needed. The more than 50 years record of the catchment Wernersbach WB did show a significant positive trend in ET, but the almost 25 years ET record of the flux tower DE-Tha did not.
- About five years of integration were applied to reduce the influence of water storage on ET sufficiently for WB. The flux tower ET shows the hourly and daily dynamics. On a monthly scale, both observations were combined to yield plausible monthly ET estimations for WB.
- On the basis of this corrected and extended database for WB, we showed that a decent amount of ET is supported only in early summer of drought years (“drought paradox”, see Teuling et al. 2013). Later in the year, the depletion of soil water leads to a collapse of ET, a situation that has become increasingly common for WB in the last two decades.
- The long-term variability of hydro-meteorological variables is clearly related to variability in regional climate, but is compensated or enlarged by effects of land use and water management. Until the 1980 s, land use effects (most importantly, forest stands damaged by acid rain) dominated and led to decreasing ET rates. Since the 1990 s, both climate (increasing atmospheric demand) and land use (improved management practices) led to an increase of actual ET. In 2010 s, climate induced damages of forest stands (due to droughts, storms, snow load, and bark beetle infestations) counteracted and led to an overall drastic decrease of ET in WB.
- On average, the systematic long-term difference in actual ET between WB and the nearby EC station DE-Tha is large (around 250 mm/yr). Strictly speaking, we conclude that ET in the footprint of the flux tower DE-Tha is not representative for WB. We did not find any large systematic bias in long-term ET data from the catchment budget for the WB setup. Primarily different site characteristics and methodological shortcomings of EC contributed to this bias. From plausibility checks based on additional measurements and modelling, we found that the contribution of site characteristics, explaining around 40–85 mm/yr, was smaller than the methodological bias, explaining around 130–180 mm/yr of the observed difference.
- The paired set up of catchment and flux tower helped to identify potential systematic shortcomings of the standard EC closure correction scheme during and after rain events. In contrast to low vegetation, lysimeters are not a realistic option for a reference of ET from tall mature forests. A small forested catchment is a potential solution, which is a striking argument for the paired catchment – flux tower concept with redundant and complementing measurements of ET.

There is a clear answer to the main question of this study concerning the impact of climate change on ET at the Tharandt Forest. While a direct positive influence on ET exists via an increasing atmospheric demand, and actual ET is increasing generally as well, there are also land-use effects, which are associated to climate change. These indirect effects of climate extremes on forest stands such as droughts, beetle infestations, wind throws etc. will have a lasting impact (memory effect), even when the climate alone returns to “normal”. The last two years of the investigated period (extremely dry and warm) could be - according to some regional climate projections - a preview of future conditions.

Further research should include simulations with physically based hydrological/land surface models, as well as a careful integration of land use/water management changes in these models. Parameterisation and understanding will profit from highly resolved remote sensing information (satellite and airborne). Finally, excellent data records will still be needed; improvements like a better EC flux tower correction included. After all, measurements will remain the benchmark for model performance. They will be necessary to isolate and judge on existing changes, and they should provide a robust reference for climate change projection of water balance components.

6. Data

Along with this paper we provide a freely available monthly hydroclimatological dataset for the period 1968–2019 and an exemplary daily dataset of the year 2017 (Pluntke et al., 2022). This dataset should foster research as well as teaching in this joint field of hydrology, ecology and climatology. Data were quality checked, homogenized and gap filled.

Funding

Important research grants included the DFG SPP”Regionalisierung in der Hydrologie” (early 1990 s), DFG SPP “MetStröm“ (2007–2013), several EU funded projects, like EUROFLUX (1996–99), TRACEFLUX (2002–04), and CarboEurope IP (2005–08); various BMBF projects as well as essential support for the flux tower infrastructure from BMBF and BMDV (ICOS), TU Dresden (funded by the Free State of Saxony), Saxon Ministry of the Environment and Agriculture, and the recent DFG grant BE 1721/23-1.

CRediT authorship contribution statement

T. Pluntke: Conceptualization, Methodology, Formal analysis, Supervision, Visualization, Writing – original draft, Writing – review & editing. **C. Bernhofer:** Conceptualization, Formal analysis, Supervision, Writing – original draft, Writing – review & editing, Funding acquisition. **T. Grünwald:** Writing – original draft. **M. Renner:** Formal analysis, Visualization, Writing – original draft, Writing – review & editing. **H. Prasse:** Writing – original draft.

Declaration of Competing Interest

The authors declare that they have no known competing financial interests or personal relationships that could have appeared to influence the work reported in this paper.

Data availability

Data are available under: http://www.hydroshare.org/resource/ca36686775a14c75bfe4ada5c51a98c5

Acknowledgements

We would like to thank Uta Moderow, Ronald Queck, Uwe Spank, Barbara Köstner, Markus Hehn, Thi Thành Luong, Stefanie Fischer (all TU Dresden, Meteorology), Kai Schwärzel (THÜNEN, Eberswalde), and numerous colleagues for discussions during the preparation of the paper as well as for their contributions to research at the Tharandt Forest. We are also especially grateful for the pioneering work of the previous holders of the Chair of Meteorology, Herrmann Pleiß, who initiated the catchment research at TU Dresden and founded the WB catchment, and Gerd Peschke, who studied soil moisture dynamics using neutron probes in WB in the 1980 s and who initiated the first measurements at the flux tower in the early 1990 s.The first instrumentation at the tower was supervised by Günter Flemming and set into operation by Horst Hebentanz. Horst Hebentanz, Uwe Eichelmann und Udo Postel also contributed immensely to the long-term operation of the catchment.

Appendix

References

Alam, S. A., Rintala, J-M., Ahlgren, K., Juurola, E., 2019. ICOS Handbook: Knowledge through observations. (Version 2 ed.) ICOS ERIC.
Allen, R., Smith, M., Perrier, A., Pereira, L., S.,, 1994. An update for the definition of reference evapotranspiration. ICID Bull. 43, 1–34.
Amiro, B.D., Wuschke, E.E., 1987. Evapotranspiration from a boreal forest drainage basin using an energy balance/eddy correlation technique. Bound.-Lay. Meteorol.. 38 (1–2), 125–139. https://doi.org/10.1007/BF00121560.
Arbeitskreis KLIWA, Stölzle, M., Blauhut, V., Kohn, I., Krumm, J., Weiler, M., Stahl, K., LUBW Landesanstalt für Umwelt, Bayerisches Landesamt für Umwelt, Rheinland-Pfalz, Landesamt für Umwelt, 2018. Low water in southern Germany: analyses, scenarios and recommendations for action (orig. title: Niedrigwasser in Süddeutschland: Analysen, Szenarien und Handlungsempfehlungen). https://www.kliwa.de/_download/KLIWAHeft23.pdf, accessed in April 2022.
Aubinet, M., Grelle, A., Ibrom, A., Rannik, Ü., Moncrieff, J., Foken, T., Kowalski, A.S., Martin, P.H., Berbigier, P., Bernhofer, C., Clement, R., Elbers, J., Granier, A., Grünwald, T., Morgenstern, K., Pilegaard, K., Rebmann, C., Snijders, W., Valentini, R., et al., 1999. Estimates of the annual net carbon and water exchange of forests: the EUROFLUX methodology. Adv. Ecol. Res. 30, 113–175. https://linkinghub.elsevier.com/retrieve/pii/S0065250408600185.
Baldocchi, D., Falge, E., Gu, L., Olson, R., et al., 2001. FLUXNET: a new tool to study the temporal and spatial variability of ecosystem-scale carbon dioxide, water vapour and energy flux densities. Bull Amer Meteor Soc 82, 2415–2435. https://doi.org/10.1175/1520-0477(2001)082<2415:FAN TTS>2.3.CO;2.
Bates, B., Kundzewicz, Z. W., IPCC (Eds.), 2008. Climate change and water. Technical Paper of the Intergovernmental Panel on Climate Change.
Bernhofer, C. (Ed.), 2002. Exkursions- Und Praktikumsführer Tharandter Wald: Material Zum "Hydrologisch-Meteorologischen Feldpraktikum". Technische Universität Dresden, Dresden. Tharandt Klimaprotok 6,ISBN 3-86005-313-2.
Bernhofer, C., Aubinet, M., Clement, R., Grelle, A., Grünwald, T., Ibrom, A., Jarvis, P., Rebmann, C., Schulze, E.-D., Tenhunen, J.D., 2003. Spruce forests (Norway and Sitka spruce, including Douglas fir): Carbon and water fluxes and balances, ecological and ecophysiological determinants. in: Valentini R. (Ed.), Fluxes of Carbon, Water and Energy of European Forests. Ecological Studies 163, 99-123.
Bernhofer, C., Franke, J., Goldberg, V., Seegert, J., W. Küchler, 2006. Regional climate change - to be included in future flood risk analysis?, in: Schanze, J.; Zeman, E.; Marsalek, J. (Eds.), Flood Risk Management: Hazards, Vulnerability and Mitigation Measures. Dordrecht: Springer, 2006, NATO Science Series - IV. Earth Environ Sci 67, 319pp.
Bernhofer, C., Goldberg, V., Franke, J., Mellentin, U., et al., (eds.), 2008. Saxony in climate change: an analysis (orig. title: Sachsen im Klimawandel: eine Analyse. Freistaat Sachsen), https://publikationen.sachsen.de/bdb/artikel/12173/documents/25586, accessed in April 2022.
Bernhofer, C., Franke, J., Fischer, S., 2015. Analyse der Klimaentwicklung in Sachsen. Schriftenreihe des LFULG 03/2015, Freistaat Sachsen, Staatsministerium für Umwelt und Landwirtschaft.
Bernhofer, C. (Ed.) (2018): Meteorologie in Dresden 1954-heute. Überblick inkl. Bibliographie. Tharandt Klimaprotok 10, TU Dresden, Dresden, ISBN 3-86005-397-3.
Budyko, M., 1974. Climate and life. Academic Press, New York, USA.
Clausnitzer, F., Köstner, B., Schwärzel, K., Bernhofer, C., 2011. Relationships between canopy transpiration, atmospheric conditions and soil water availability—analyses of long-term sap-flow measurements in an old Norway spruce forest at the Ore Mountains/Germany. Agric. For. Meteorol. 151, 1023–1034. https://doi.org/10.1016/j.agrformet.2011.04.007.
Dyck, S., Peschke, G., 1995. Grundlagen der Hydrologie. Verlag für Bauwesen.
Falge, E., Baldocchi, D., Olson, R.J., Anthoni, P., Aubinet, M., Bernhofer, C., Burba, G., Ceulemans, R., Clement, R., Dolman, H., Granier, A., Gross, P., Grünwald, T., Hollinger, D., Jensen, N.-O., Katul, G., Keronen, P., Kowalski, A., Ta, C., Lai, Law, B. E., Meyers, T., el, al.,, 2001. Gap filling strategies for longterm energy flux data sets, a short communication. Agric. Forest Meteorol. 107, 71–77.
Federer, C. A., 2021. The BROOK90 Hydrologic Model, www.ecoshift.net/brook/brook90.htm, accessed in January 2022.
Fernández-Martínez, M., Vicca, S., Janssens, I.A., Ciais, P., Obersteiner, M., Bartrons, M., Sardans, J., Verger, A., Canadell, J.G., Chevallier, F., Wang, X., Bernhofer, C., Curtis, P.S., Gianelle, D., Grünwald, T., Heinesch, B., Ibrom, A., Knohl, A., Laurila, T., et al., 2017. Atmospheric deposition, CO2, and change in the land carbon sink. Sci. Rep. 7 (1) https://doi.org/10.1038/s41598-017-08755-8.
Fischer, S., Moderow, U., Gliksman, D., Bernhofer, C., 2022. Evaporation of Intercepted Rainfall - Comparing Canopy Water Budget and Energy Balance Related Long Term Measurements at a Norway Spruce Site. Submitted to Agric. Forest Meteorol.
Foken, T., 2008. The energy balance closure problem: an overview. Ecol. Appl. 18, 1351–1367. https://doi.org/10.1890/06-0922.1.
Frühauf, C., Zimmermann, L., Bernhofer, C., 1999. Comparison of forest evapotranspiration from ECEB-measurements over a Spruce stand with the water budget of a catchment. Phys. Chem. Earth 24 (7), 805–808.
Gielen, B., Acosta, M., Altimir, N., Buchmann, N., Cescatti, A., Ceschia, E., Fleck, S., Hörtnagl, L., Klumpp, K., Kolari, P., Lohila, A., Loustau, D., Marańon-Jimenez, S., Manise, T., Matteucci, G., Merbold, L., Metzger, C., Moureaux, C., Montagnani, L., et al., 2018. Ancillary vegetation measurements at ICOS ecosystem stations. Int. Agrophys. 32 (4), 645–664. https://doi.org/10.1515/intag-2017-0048.
Graf, A., Bogena, H.R., Drüe, C., Hardelauf, H., Pütz, T., Heinemann, G., Vereecken, H., 2014. Spatiotemporal relations between water budget components and soil water content in a forested tributary catchment. Water Resour. Res. 50, 4837–4857. https://doi.org/10.1002/2013WR014516.
Graf, A., Klosterhalfen, A., Arriga, N., Bernhofer, C., Bogena, H., Bornet, F., Brüggemann, N., Brümmer, C., Buchmann, N., Chi, J., Chipeaux, C., Cremonese, E., Cuntz, M., Dušek, J., El-Madany, T.S., Fares, S., Fischer, M., Foltýnová, L., Gharun, M., 2020. Altered energy partitioning across terrestrial ecosystems in the European drought year 2018. Philos. Trans. Royal Soc. B: Biol. Sci. 375 (1810) https://doi.org/10.1098/rstb.2019.0524.
Grunicke, S., Queck, R., Bernhofer, C., 2020. Long-term investigation of forest canopy rainfall interception for a spruce stand. Agric. For. Meteorol. 292–293 https://doi.org/10.1016/j.agrformet.2020.108125.
Grünwald, T., Bernhofer, C., 2007. A decade of carbon, water and energy flux measurements of an old spruce forest at the Anchor Station Tharandt. Tellus B: Chem Phys Meteorolo 59 (3), 387–396. https://doi.org/10.1111/j.1600-0889.2007.00259.x.
IPCC, 2014. Climate change 2014: impacts, adaptation, and vulnerability: Working Group II contribution to the fifth assessment report of the Intergovernmental Panel on Climate Change (C. B. Field, V. R. Barros, & Intergovernmental Panel on Climate Change (Eds.), Cambridge University Press.
Jones, P., Moberg, A., 2003. Hemispheric and large-scale surface air temperature variations: An extensive revision and an update to 2001. J. Climatol. 16, 206–223. https://doi.org/10.1175/1520-0442(2003)016<0206:HALSSA>2.0.CO;2.
Karbaum, H., 1969. Der Niederschlag als Wasserhaushaltsgröße. Abhandlungen des MD der DDR 86/ XI, 3–78.

Kendall, M.G., 1955. Rank Correlation Methods. Griffin, London.
Kljun, N., Calanca, P., Rotach, M.W., Schmid, H.P., 2004. A Simple Parameterisation for Flux Footprint Predictions. Boundary-Layer Meteorol 112, 503–552. https://doi.org/10.1023/B:BOUN.0000030653.71031.96.
Kolář, T., Čermák, P., Oulehle, F., Trnka, M., Štěpánek, P., Cudlín, P., Hruška, J., Büntgen, U., Rybníček, M., 2015. Pollution control enhanced spruce growth in the "Black Triangle" near the Czech-Polish border. Sci. Total Environ. 538, 703–711. https://doi.org/10.1016/j.scitotenv.2015.08.105.
Körner, P., Kalaß, D., Kronenberg, R., Bernhofer, C., 2020. REAL-Fog: A simple approach for calculating the fog in the atmosphere at ground level. Meteorol. Z. 29 (1), 55–65. https://doi.org/10.1127/metz/2019/0976.
Köstner, B., 2001. Evaporation and transpiration from forests in Central Europe - relevance of patch-level studies for spatial scaling. Meteorol Atmospheric Phys 76 (1–4), 69–82. https://doi.org/10.1007/s007030170040.
Kosugi, Y., Katsuyama, M., 2007. Evapotranspiration over a Japanese cypress forest. II. Comparison of the eddy covariance and water budget methods. J. Hydrol. 334 (3–4), 205–311. https://doi.org/10.1016/j.jhydrol.2006.05.025.
Kottek, M., Grieser, J., Beck, C., Rudolf, B., Rubel, F., 2006. World Map of the Köppen-Geiger climate classification updated. Meteorol. Z. 15, 259–263. https://doi.org/10.1127/0941-2948/2006/0130.
Kundzewicz, Z.W., Pińskwar, I., Brakenridge, G.R., 2013. Large floods in Europe, 1985–2009. Hydrol. Sci. J. 58 (1), 1–7. https://doi.org/10.1080/02626667.2012.745082.
Luong, T.T., Pöschmann, J., Kronenberg, R., Bernhofer, C., 2021. Rainfall threshold for flash flood warning based on model output of soil moisture: case study Wernersbach, Germany. Water 2021 (13), 1061. https://doi.org/10.3390/w13081061.
Mann, H.B., 1945. Nonparametric tests against trend. Econometrica 13, 245–259.
Mauder, M., Foken, T., Cuxart, J., 2020. Surface-energy-balance closure over land: a review. Boundary-Layer Meteorol. 177, 395–426. https://doi.org/10.1007/s10546-020-00529-6.
Mellmann, P., Grünwald, T., Frühauf, C., Podlasly, C., Bernhofer, C., 2003. An objective method for creating a representative stand parameter set using source area analysis for the Tharandt Forest anchor station (orig. title: Eine objektive Methode zur Erstellung eines repräsentativen Bestandesparametersatzes mit Hilfe der Quellflächen-Analyse für die Ankerstation Tharandter Wald). In: Bernhofer, C. (Ed.), Tharandt Klimaprotok 8, 29-54, Technische Universität Dresden.
Mauder, M., Ibrom, A., Wanner, L., De Roo, F., Brugger, P., Kiese, R., Pilegaard, K., 2021. Options to correct local turbulent flux measurements for large-scale fluxes using an approach based on large-eddy simulation. Atmos. Meas. Tech. 14 (1), 7835–7850. https://doi.org/10.5194/amt-14-7835-2021.
Moderow, U., Bernhofer, C., 2014. Cluster of the Technische Universität Dresden for greenhouse gas and water fluxes. In: ILEAPS-Newsletter, Special Issue on Environmental Research Infrastructures, pp. 34–37.
Müller, G., 1998. On the spatial variability of runoff formation in low mountain ranges - process studies for an area classification according to typical runoff contributions (orig. title: Zur räumlichen Variabilität der Abflussbildung im Mittelgebirge - Prozessstudien für eine Flächenklassifkation nach typischen Abflussbeiträgen). Dissertation at Technische Universität Dresden.
Murray, M., 1967. On the computation of saturation vapor pressure. J. Appl. Meteorol. 6 (1, 203).
Panin, G.N., Bernhofer, C., 2008. Parametrization of Turbulent Flux over Inhomogeneous Landscapes. Atmosph Ocean Phys 44, 701–716.
Pastorello, G., Trotta, C., Canfora, E., Chu, H., Christianson, D., Cheah, Y.-W., Poindexter, C., Chen, J., Elbashandy, A., Humphrey, M., Isaac, P., Polidori, D., Ribeca, A., van Ingen, C., Zhang, L., Amiro, B., Ammann, C., Arain, M. A., Ardö, J., et al., 2020. The FLUXNET2015 dataset and the ONEFlux processing pipeline for eddy covariance data. Scientific Data 7(1), https://doi.org/10.1038/s41597-020-0534-3.
Peschke, G., Etzenberg, C., Müller, G., Töpfer, J., Zimmermann, S., 1999. Runoff Generation Regionalization - analysis and a Possible approach to a Solution. University of Braunschweig, Germany.
Petrescu, A.M.R., Lohila, A., Tuovinen, J.-P., Baldocchi, D.D., Desai, A.R., Roulet, N.T., Vesala, T., Dolman, A.J., Oechel, W.C., Marcolla, B., Friborg, T., Rinne, J., Matthes, J.H., Merbold, L., Meijide, A., Kiely, G., Sottocornola, M., Sachs, T., Zona, D., et al., 2015. The uncertain climate footprint of wetlands under human pressure. Proc. Natl. Acad. Sci. 112 (15), 4594–4599. https://doi.org/10.1073/pnas.1416267112.
Philipona, R., Behrens, K., Ruckstuhl, C., 2009. How declining aerosols and rising greenhouse gases forced rapid warming in Europe since the 1980s: AEROSOL VERSUS GREENHOUSE GAS FORCING. Geophys. Res. Lett. 36 (2) https://doi.org/10.1029/2008GL036350.
Ploberger, W., Krämer, W., 1992. The CUSUM Test with OLS Residuals. Econometrica 60 (2), 271–285.
Pluntke, T., Bernhofer, C., Grünwald, T., 2022. Hydrometeorological observations for the catchment Wernersbach (Germany) and Eddy Covariance observations of two nearby EC towers. HydroShare. http://www.hydroshare.org/resource/ca36686775a14c75bfe4ada5c51a98c5.
Pluntke, T., Kronenberg, R., Hänsel, S., Rumpf, D., Zimmermann, F., Matschullat, J., Bernhofer, C., 2021. Erfassung und Abschätzung von Trockenheitsmerkmalen in Sachsen Erarbeitung von Optionen zur Erfassung und Abschätzung der zeitlichen Entwicklung von Trockenheitsmerkmalen für sich ändernde Klimabedingungen im Freistaat Sachsen. Schriftenreihe des LFULG 1/2021, https://publikationen.sachsen.de/bdb/artikel/36871/documents/58232, accessed April 2022.
Reichstein, M., et al., 2005. On the separation of net ecosystem exchange into assimilation and ecosystem respiration: review and improved algorithm. Glob. Chang. Biol. 11, 1424–1439. https://doi.org/10.1111/j.1365-2486.2005.001002.x.
Renner, M., Bernhofer, C., 2011. Long term variability of the annual hydrological regime and sensitivity to temperature phase shifts in Saxony/Germany. Hydrol. Earth Syst. Sci. 15, 1819–1833. https://doi.org/10.5194/hess-15-1819-2011.
Renner, M., Brust, K., Schwärzel, K., Volk, M., Bernhofer, C., 2014. Separating the effects of changes in land cover and climate: a hydro-meteorological analysis of the past 60 yr in Saxony. Germany. Hydrol Earth Syst Sci 18 (1), 389–405. https://doi.org/10.5194/hess-18-389-2014.
Richter, D., 1995. Results of methodical investigations for the correction of the systematic measuring error of the Hellmann precipitation gauge (orig. title: Ergebnisse methodischer Untersuchungen zur Korrektur des systematischen Meßfehlers des Hellmann-Niederschlagmessers). Berichte des Deutschen Wetterdienstes 194, Selbstverlag des Deutschen Wetterdienstes.
Sabbatini, S., Mammarella, I., Arriga, N., Fratini, G., Graf, A., Hörtnagl, L., Ibrom, A., Longdoz, B., Mauder, M., Merbold, L., Metzger, S., Montagnani, L., Pitacco, A., Rebmann, C., Sedlák, P., Šigut, L., Vitale, D., Papale, D., 2018. Eddy covariance raw data processing for CO2 and energy fluxes calculation at ICOS ecosystem stations. Intern Agrophys 32 (4), 495–515. https://doi.org/10.1515/intag-2017-0043.
Schaller, A.S., Franke, J., Bernhofer, C., 2020. Occurrence frequency of heavy precipitation in Saxony Meteorol Z 29 (5), 335–348. https://doi.org/10.1127/metz/2020/0771.
Schwarze, R., 2002. Analyse des Ablusskomponenten- und Verweilzeitregimes des Wernersbaches. In: Bernhofer, C. (Ed.), Exkursions- und Praktikumsführer Tharandter Wald. Tharandt Klimaprotok 6, 149–164, TU Dresden, ISBN 3-86005-313-2.6.
Schwärzel, K., Feger, K.H., Häntzschel, J., Menzer, A., Spank, U., Clausnitzer, F., Köstner, B., Bernhofer, C., 2009. novel approach in model-based mapping of soil water conditions at forest sites. For Ecol Manag 258, 2163–2174. https://doi.org/10.1016/J.FORECO.2009.03.033.
Seneviratne, S. I., Lehner, I., Gurtz, J., Teuling, A. J., Lang, H., Moser, U., Grebner, D., Menzel, L., Schroff, K., Vitvar, T., Zappa, M., 2012. Swiss prealpine Rietholzbach research catchment and lysimeter: 32 year time series and 2003 drought event: RIETHOLZBACH 32 YEAR SERIES AND 2003 DROUGHT. Water Resour Res 48(6), https://doi.org/10.1029/2011WR011749.
SMUL, 2019. Forest Status Report 2019 (orig. title: Waldzustandsbericht 2019). https://publikationen.sachsen.de/bdb/artikel/34742, accessed in February 2022.
Spank, U. (2010). Site Water Budget: Influences of Measurement Uncertainties on Measurement Results and Model Results. Dissertation at Technische Universität Dresden. Available via dialog: http://nbn-resolving.de/urn:nbn:de:bsz:14-qucosa-62557.
Teuling, A.J., Hirschi, M., Ohmura, A., Wild, M., Reichstein, M., Ciais, P., Buchmann, N., Ammann, C., Montagnani, L., Richardson, A.D., Wohlfahrt, G., Seneviratne, S.I., 2009. A regional perspective on trends in continental evaporation: EVAPORATION TRENDS. Geophys. Res. Lett. 36 (2) https://doi.org/10.1029/2008GL036584.
Teuling, A.J., Seneviratne, S.I., Stöckli, R., Reichstein, M., Moors, E., Ciais, P., Luyssaert, S., van den Hurk, B., Ammann, C., Bernhofer, C., Dellwik, E., Gianelle, D., Gielen, B., Grünwald, T., Klumpp, K., Montagnani, L., Moureaux, C., Sottocornola, M., Wohlfahrt, G., 2010. Contrasting response of European forest and grassland energy exchange to heatwaves. Nat. Geosci. 3 (10), 722–727. https://doi.org/10.1038/ngeo950.
Teuling, A.J., Van Loon, A.F., Seneviratne, S.I., Lehner, I., Aubinet, M., Heinesch, B., Bernhofer, C., Grünwald, T., Prasse, H., Spank, U., 2013. Evapotranspiration amplifies European summer drought. Geophys. Res. Lett. 40 (10), 2071–2075. https://doi.org/10.1002/grl.50495.
Teuling, A.J., de Badts, E.A.G., Jansen, F.A., Fuchs, R., Buitink, J., Hoek van Dijke, A.J., Sterling, S.M., 2019. Climate change, reforestation/afforestation, and urbanization impacts on evapotranspiration and streamflow in Europe. Hydrol. Earth Syst. Sci. 23 (9), 3631–3652. https://doi.org/10.5194/hess-23-3631-2019.
Tomer, M., Schilling, K., 2009. A simple approach to distinguish landuse and climate-change effects on watershed hydrology. J. Hydrol. 376, 24–33. https://doi.org/10.1016/j.jhydrol.2009.07.029.
Tröger, M., 2012. Evaluation of biotope types and land use mapping (orig. title: Auswertung der Biotoptypen und Landnutzungskartierung). accessed April 2022 Schriftenreihe des LFULG 38. https://publikationen.sachsen.de/bdb/artikel/12903/documents/26738,.
Valentini, R., Matteucci, G., Dolman, A.J., Schulze, E.-D., Rebmann, C., Moors, E.J., Granier, A., Gross, P., Jensen, N.O., Pilegaard, K., Lindroth, A., Grelle, A., Bernhofer, C., Grünwald, T., Aubinet, M., Ceulemans, R., Kowalski, A.S., Vesala, T., Rannik, Ü., et al., 2000. Respiration as the main determinant of carbon balance in European forests. Nature 404 (6780), 861–865. https://doi.org/10.1038/35009084.
Van Dijk, A.I.J.M., Gash, J.H., van Gorsel, E., Blanken, P.D., Cescatti, A., Emmel, C., Gielen, B., Harman, I.N., Kiely, G., Merbold, L., Montagnani, L., Moors, E., Sottocornola, M., Varlagin, A., Williams, C.A., Wohlfahrt, G., 2015. Rainfall interception and the coupled surface water and energy balance. Agric. For. Meteorol. 214–215, 402–415. https://doi.org/10.1016/j.agrformet.2015.09.006.
Vorobevskii, I., Luong, T.T., Kronenberg, R., Grünwald, T., Bernhofer, C., 2022. Modelling evaporation with local, regional and global BROOK90 frameworks: importance of parameterization and forcing. Hydrol. Earth Syst. Sci. Discuss. 26, 3177–3239. https://doi.org/10.5194/hess-26-3177-2022.
Westphal, M., 2007. Classification of the terrain-dependent wind distribution in the Tharandt Forest by means of the diagnostic wind model WITRAK (orig. title: Klassifizierung der geländeabhängigen Windverteilung im Tharandter Wald mittels des diagnostischen Windmodells WITRAK). Technische Universität Dresden. Diploma thesis.
Wild, M., 2005. From dimming to brightening: decadal changes in solar radiation at earth's surface. Science 308 (5723), 847–850. https://doi.org/10.1126/science.1103215.

Wutzler, T., 2002. Establishment of a data model for the quantification of the carbon stocks of the Tharandt Forest (orig. title: Aufstellung eines Datenmodelles zur Quantifizierung der Kohlenstoffvorräte des Tharandter Waldes). Technische Universität Dresden. Diploma thesis.
WWDR (United Nations World Water Development Report), 2020. Water and Climate Change. UNESCO, Paris.
Yao, Y., Liang, S., Li, X., Liu, S., Chen, J., Zhang, X., Jia, K., Jiang, B., Xie, X., Munier, S., Liu, M., Yu, J., Lindroth, A., Varlagin, A., Raschi, A., Noormets, A., Pio, C., Wohlfahrt, G., Sun, G., et al., 2016. Assessment and simulation of global terrestrial latent heat flux by synthesis of CMIP5 climate models and surface eddy covariance observations. Agric. For. Meteorol. 223, 151–167. https://doi.org/10.1016/j.agrformet.2016.03.016.
Zeileis, A., Leisch, F., Hornik, K., Kleiber, C., 2002. strucchange: an R package for testing for structural change in linear regression models. J. Stat. Softw. 7 (2).